JOURNAL OF MORPHOLOGY 277:786–813 (2016)

Development and Morphological Variation of the Axial and Appendicular Skeleton in Hylidae (Lissamphibia, Anura)

Mónica Soliz[1] and María Laura Ponssa[2]*

[1]*Facultad de Ciencias Naturales, Universidad Nacional de Salta, Cátedra Vertebrados, Avenida Bolivia 5150, Salta Capital, Argentina*
[2]*Unidad Ejecutora Lillo (UEL). CONICET—Fundación Miguel Lillo, Miguel Lillo 251. S.M. de Tucumán (4000), Tucumán, Argentina*

ABSTRACT The axial and appendicular skeleton, the associated musculature and tendons form a functional system related to specific modes of locomotion in anurans. Many transformations in the structures linked with the locomotor function of the adult occur during larval stages and metamorphosis. In this study, we present the larval ontogeny and adult morphology of the axial and appendicular skeletons of 14 species of frogs in the family Hylidae with different locomotor modes and habitat uses. Among Hylidae, a diversity of shapes, locomotory types occurs (e.g., walker, swimmer, jumper, hopper) and different habitat types occupied (shrubby, terrestrial, aquatic, arboreal). Many elements complete differentiation at the end of metamorphosis; others, such as sesamoids, still show an incomplete development at that stage. Sixty seven characters were scored and optimized in an available phylogeny. Nine characters of developmental timing and adult osteology are optimized as synapomorphies of specific groups. Some characters appear to be related to the locomotor type (e.g., the sacro-urostyle region configuration is highly linked with the jumping mode; nonexpanded diapophyses would related to aquatic habitat use). Nevertheless, the functional interpretations are quite particular to this family. Monophyletic clades are also groups with shared locomotory modes or habitat uses. Hence, the hypothesis of common ancestry or adaptation can be evaluated, taking into account the analysis level of the phylogenetic context, so that, when a character is inherited via common ancestry, it necessarily means that functional constraints could also be inherited. Here, we outline the basis for further work on: postmetamorphic development as a fundamental period for the complete differentiation of structures related to a full locomotor functionality; the biomechanical performance in relationship to the variation in ligaments and sesamoids; the importance of analyzing these topics within the frame of heterochrony. J. Morphol. 277:786–813, 2016.

KEY WORDS: skeleton; postcranial; anuran; metamorphosis

INTRODUCTION

The axial and appendicular skeleton and the associated musculature and tendons form a functional system related to locomotory modes in anurans (Emerson and De Jongh, 1980; Rage and Roček, 1989; Jenkins and Shubin, 1998; Přikryl et al. 2009; Reilly and Jorgensen, 2011). Several postcranial characters of this system have been studied using morpho-functional criteria (Emerson, 1988), e.g., length of the ilium and size of dorsal iliac crest, length of the hindlimb, length and orientation of the presacral transverse process, length, shape, and orientation of the sacral diapophyses, presence and development of neural spines, and types of iliosacral articulation (Emerson, 1979, 1982, 1984; Trueb, 1973; Van Dijk, 2002; Manzano and Barg, 2005; Simons, 2008; Reilly and Jorgensen, 2011). Emerson (1979) examined the iliosacral articulation in anurans and identified three aspects of postcranial morphology that belong to a single functional complex, that is, the relative length of the ilia, the relative length of the posterior transverse processes, and characteristics of the dorsal iliac crest. Reilly and Jorgensen (2011) scored two new traits related to pelvic function, that is, the form of the sacro-urostylic articulation, and the dorsal ridge on the urostyle. They also presented a new pattern for the evolution of pelvic systems and locomotor modes in frogs, concluding that the

Additional Supporting Information may be found in the online version of this article.

Contract grant sponsor: CONICET; Contract grant numbers: PIP 284 and PIP 875; Contract grant sponsor: FONCyT; Contract grant number: PICT 2013-0404; Contract grant sponsor: UNSa; Contract grant number: Proy.1851/10.

*Correspondence to: María Laura Ponssa; Fundación Miguel Lillo. Miguel Lillo 251. S.M. de Tucumán (4000), Tucumán, Argentina. E-mail: mlponssa@hotmail.com

Received 17 July 2015; Revised 19 February 2016; Accepted 27 February 2016.

Published online 24 March 2016 in Wiley Online Library (wileyonlinelibrary.com). DOI 10.1002/jmor.20536

TABLE 1. Locomotor mode and habitat use of the species included in this study

Species	Family	Locomotor mode (habitat)	Reference
Dendropsophus nanus	Hylidae	Jumper (shrubby)	Pers. Obs.
Hypsiboas pulchellus	Hylidae	Jumper (arboreal, shrubby)	Gallardo (1993)
Hypsiboas raniceps	Hylidae	Jumper (arboreal, shrubby)	Pers. Obs.
Hypsiboas riojanus	Hylidae	Jumper (arboreal, shrubby)	(Fabrezi et al., 2014)
Leptodactylus fuscus	Leptodactylidae	Jumper (terrestrial)	Ponssa (2008)
Lysapsus limellum	Hylidae	Swimmer and jumper (water and aquatic vegetation)	Manzano and Barg (2005)
Pleurodema cinereum	Leptodactylidae	Hopper (semi-terrestrial)	Vellard (1954), Lavilla
Phyllomedusa azurea	Hylidae	Walker (arboreal, shrubby)	Wells (2007)
Phyllomedusa boliviana	Hylidae	Walker (arboreal, shrubby)	Wells (2007)
Phyllomedusa sauvagii	Hylidae	Walker (arboreal)	Wells (2007); Fabrezi et al. (2014)
Phyllomedusa tetraploidea	Hylidae	Walker (arboreal, shrubby)	Manzano et al. (2004), Pombal and Haddad (1992), Wells (2007)
Pseudis platensis	Hylidae	Swimmer and jumper (water)	Manzano and Barg (2005)
Rhinella major	Bufonidae	Walker (terrestrial)	Vellard (1954), Wells, 2007
Scinax acuminatus	Hylidae	Jumper (terrestrial, shrubby, arboreal)	Pers. Obs.
Scinax fuscovarius	Hylidae	Jumper (terrestrial, shrubby, arboreal)	Fabrezi et al. (2014)
Scinax nasicus	Hylidae	Jumper (terrestrial, arboreal, shrubby)	Pers. Obs.
Telmatobius atacamensis	Telmatobiidae	Walker (aquatic)	Lavilla (1988), Lavilla and Barrionuevo (2005), Vellard (1954), Wells (2007)
Telmatobius ceiorum	Telmatobiidae	Walker (semiaquatic)	Cei (1980), Laurent (1970), Lavilla (1988), Lavilla and Barrionuevo (2005), Vellard (1954), Wells (2007)
Trachicephalus typhonius	Hylidae	Jumper (arboreal)	Pers. Obs.

lateral-bender and walker/hopper condition are basal and generally conserved in Anura. Reilly and Jorgensen (2011) included 12 species of hylids. More recently, these authors stated that limb morphology was not significantly different across most locomotor modes (Jorgensen and Reilly, 2013). Many of the developmental and evolutionary transformations in the structures linked with locomotor function occur throughout larval stages and metamorphosis in anurans (Ročkova and Roček, 2005; Púgener and Maglia, 2009; Přikryl et al., 2009; Fabrezi, 2011; Manzano et al., 2013; Fabrezi et al., 2014).

The family Hylidae includes approximately 900 species that are grouped in three subfamilies and 50 genera (Faivovich et al., 2005; Wiens et al., 2010; Pyron and Wiens, 2011). Hylidae have been characterized by possessing claw-shaped terminal phalanges and the three articular surfaces on metacarpal III (Duellman, 2001). Most hylid taxa are arboreal, although there are terrestrial and aquatic forms, which involve different locomotor modes (hopping, jumping, swimming, walking; Jorgensen and Reilly, 2013). Simons (2008) proposed that specific morphometric pattern linked with locomotion may not extend to all anurans, but they can be identifiable in particular clades. Studies addressing the link between postcranial morphology and mode of locomotion in hylids were conducted in adult specimens of several species (Emerson, 1979, 1982, 1988; Simons, 2008; Reilly and Jorgensen, 2011) and also through the ontogeny of some species (Sheil and Alamillo, 2005; Maglia et al., 2007; Fabrezi and Goldberg, 2009; Púgener and Maglia, 2009; Manzano et al., 2013).

Here, we describe the larval ontogeny and adult morphology of the axial and appendicular skeletons for 14 species within the Hylidae with different locomotor modes and habitats. We discuss the evolution of some interesting characters and their relationship with locomotor mode in a phylogenetic context.

MATERIALS AND METHODS

We examined the skeleton of the vertebral column, pectoral and pelvic girdles in a larval series for eight species representing five genera: *Hypsiboas riojanus* (Koslowsky, 1895), *Lysapsus limellum* (Cope, 1862), *Phyllomedusa azurea* (Cope, 1862), *Phyllomedusa boliviana* (Boulenger, 1902), *Phyllomedusa sauvagii* (Boulenger, 1882), *Pseudis platensis* (Gallardo, 1961), *Scinax acuminatus* (Cope, 1862), and *Scinax fuscovarius* (Lutz, 1925). In addition, adult specimens of these and others species [*Dendropsophus nanus* (Boulanger, 1889), *Hypsiboas pulchellus* (Duméril and Bibron, 1841), *Hypsiboas raniceps* (Cope, 1862), *Phyllomedusa tetraploidea* (Pombal and Haddad, 1992), *Scinax nasicus* (Cope, 1862), *Trachycephalus typhonius* (Linnaeus, 1758)], and species of other families [*Leptodactylus fuscus* (Schneider, 1799), *Pleurodema cinereum* (Cope, 1878), *Rhinella major* (Müller and Helmich, 1936), *Telmatobius ceiorum* (Laurent, 1970), *Telmatobius atacamensis* (Gallardo, 1962)] were used as comparison. The species were assigned to different locomotor modes and habitat uses (Table 1). Locomotory modes were classified as jumper, hopper, walker, or swimmer (Table 1). According to the habitat, species were classified as arboreal if they regularly occured on trees; shrubby, if they occured in bushes, low-growing vegetation as grasses, bromeliads, and so forth; terrestrial, if they live on land next to swamp or ponds or in slopes; aquatic, if they are usually found in water. A total of 170 tadpoles (Stages 26–46) and 22 adult specimens were used (material deposited in Insituto de

Herpetología, Fundación Miguel Lillo; Laboratorio de Genética Evolutiva, Universidad Nacional de Misiones; Museo de Ciencias Naturales, Universidad Nacional de Salta; Argentina; a complete list of the material including sample size and catalogue numbers is given in supporting information; Appendix I). Specimens were staged according to Gosner (1960). To obtain the developmental series, larvae were hatched or collected and reared in appropriate semicaptive conditions (Field permit Exp.227-53558/10-Res.000161, Secretaría de Medio Ambiente de la Pcia. de Salta, Argentina). The tadpoles were placed in plastic containers, 10 larvae by 1 liter of water, and fed with fish pellets brand *Shullet ad libitum*. The water was changed every couple of days. The light and temperature conditions were the natural in summer (about 13 hrs of light per day and an average temperature of 32°C). The larvae were raised from January to March, 2013. The tadpoles were anesthetized and killed with lidocane. Samples were fixed at appropriate intervals during development (Mc Diarmid and Altig, 1996; Heyer et al., 2001). All specimens were double-stained with Alcian Blue and Alizarin Red, and subsequently cleared (Wassersug, 1976). Observations and illustrations were performed using a Zeiss Discovery V8 stereoscope with a Nikon Coolpix P6000, 5-megapixel digital camera. Terminology of the skeletal structures and character definition follows Trueb (1973), Emerson (1979), Duellman and Trueb (1994), Rocoková and Roček (2005), Maglia et al. (2007), Púgener and Maglia (2009) and Ponssa et al. (2010). Measurements and angles were assessed using the software Image Tool (Wilcox et al., 2002; supporting information Appendix II).

Histological preparations of articular areas of both pectoral and pelvic girdles in *H. riojanus*, *L. limellum*, and *P. sauvagii* (Appendix I) were obtained to detect variability in the joint areas, where movement could be considered a mechanobiological stimulus. The formalin-fixed specimens were dehydrated with graded alcohols and cleared in xylene. Serial sections were cut on an MSE sledge microtome (Microscopía Electrónica del Noroeste Argentino, LAMENOA). The following sections were performed: in the pectoral girdle, transversal cut in anteroposterior sense; in the pelvic girdle, frontal cuts in ventrodorsal sense; in the iliosacral region, transverse sections in adults and frontal sections in metamorphic individuals. Histological serial sections (6 μm thick) of paraffin-embedded tissues were stained with Alcian blue-hematoxylin-eosin (modified from Totty, 2002). Terminology for the tissue of the pectoral girdle follows Baleeva (2001, 2009), Kaplán (2000, 2004); terminology of pelvic girdle follows Manzano and Barg (2005); Shearman (2005), Přikryl et al. (2009), and Manzano et al. (2013).

Phylogenetic Mapping

Twenty eight larval characters and 40 adult characters were included in a matrix (Appendix III). Larval character states were coded based on developmental stages (Gosner, 1960): (0) Larval I, Stages 26 to 30; (1) Larval II, Stages 31 to 33; (2) Larval III, Stages 34 to 37; (3) Larval IV, Stages 38 to 41; (4) Early metamorphic, Stages 42 to 44; (5) Late metamorphic, Stages 45 and 46. The characters were optimized, using parsimony, in the phylogenetic hypothesis proposed by Pyron and Wiens (2011). We analyzed our data with the software TNT (Goloboff et al. 2008), and only considered unambiguous changes. The resulting cladogram was edited using Winclada software 1.00.08 (Nixon, 2002).

RESULTS

We detected some difference in the timing of developmental events among species (Table 2). Quantitative measurements taken from eight adult hylids are given in supporting information Appendix II.

Scinax Species

Our description of the ontogenic and adult pattern is based on *Scinax acuminatus*, with references to the characters that show differences in *S. fuscovarius*.

Ontogeny. Between Stages 20 and 31, one sacral and one postsacral vertebral element are present (Fig. 1A). At Stages 28–30, eight presacral vertebrae are evident (Fig. 1A). At Stage 32, the girdles and limb buds are visible. At Stage 34, the elements of the pectoral girdle, scapula and procoracoid are visible. At Stage 35, the coracoids appear and the first pair of postsacral vertebral elements begins to ossify. At Stage 37, the hypochord begins to chondrify (Fig. 1B) and scapula, coracoid, clavicle and cleithrum begin to ossify. At Stages 38–40, the sacral diapophyses begin to develop; chondrification of the second postsacral vertebral element occurs. The second pair of postsacral vertebral elements begin ossification, both pelvic hemigirdles contact each other at the level of ischium; the sacral diapophyses begin to develop. At Stage 41, ossification of the hypochord begins (Fig. 1C); the outline of the projection of the suprascapula is evident (Fig. 1F); the contact between both pelvic hemigirdles at the level of ischium occurs (Fig. 1I) and the typical adult shape of the posterior region of the pelvic girdle is evident. At Stage 42, the sacral diapophyses are posteriorly oriented and ossification begins; the contact between both hemipelvic girdles is completed (Fig. 1J); the ischium begins to ossify; the femur is already in a more anterior location (Fig. 1J); the anterior end of the ilium reaches the level of the presacral vertebrae-sacrum articulation and the hole in the sacral region is not present; the development of the sternum begins. At Stage 43, the second pair of spinal foramina and the third pair of postsacral vertebral elements appear; the anterior ends of the ilia articulate with the sacral diapophyses, and a cartilaginous sesamoid appears between both elements; the omosternum and the epicoracoid horns begin development (Fig. 1G). At Stage 46, the contact between hypochord and postsacral vertebral elements is completed, the anterior end of the hypochord does not exceed the level of the anterior end of the first pair of postsacral vertebral elements, the ossification of the postsacral vertebrae is completed, the sacral diapophyses are expanded (Fig. 1D), the coracoids still are not parallel to each other (Fig. 1H).

Variation to the described pattern as observed in *Scinax fuscovarius* are: Stage 34, the first pair of postsacral vertebrae are chondrified and, in the pelvic girdle, the ilium and ischium appear as separate structures (Fig. 2A). Stage 36, the first pair of postsacral vertebral elements and the illia begin to ossify. Stage 37, the second postsacral vertebral element is chondrified (Fig. 2B). Stage 38–42, the second pair of postsacral vertebral elements begin

TABLE 2. Developmental chronology of the axial and appendicular skeleton in hylids expressed in Gosner (1960) stages

Developmental event	*Hypsiboas riojanus*	*Lysapsus limellum*	*Phyllomedusa azurea*	*Phyllomedusa boliviana*	*Phyllomedusa sauvagii*	*Pseudis platensis*	*Scinax acuminatus*	*Scinax fuscovarius*
Beginning of chondrification of eighth presacral element	26*	26*	31*	36*	29	—	27*	27*
Beginning of chondrification of sacrum	26*	27	31*	36*	33*	—	29	27
Beginning of chondrification of first pair of postsacral elements	27	33*	31*	36*	33*	28*	29	34
Beginning of chondrification of girdles and limbs	33	33*	36*	36*	34	26	32	34
Beginning of chondrification of second pair of postsacral elements	33	35	36	36*	37	—	40*	36
Beginning of chondrification of hypochord	35	40	36*	36*	37	28*	37	37
Beginning of ossification of first pair of postsacral elements	33	40	36*	36*	38	37*	34	38
Beginning of ossification of coracoids	37	39	39*	—	40	37*	37	37
Beginning of ossification of scapula	36	—	36*	36*	36	37*	37	37
Beginning of ossification of second pair of postsacral elements	35	—	41	36*	43	—	41	40
Beginning of ossification of hypochord	38	40	39	36	41	26	41	41
Rotation of ilia: angle of 45° relative to axis of the body	38	40	41	—	41	—	43	41
Clavicle and cleithrum start to ossify	36	39	38	36*	37	37*	37	37
Beginning of development of sacral diapophyses	35	39	39	41*	37	—		38
IS: ischia in touch	38	40	41	41*	40	—	40*	38
Beginning of differentiation of suprascapula	38	39	42	43	37	37*	40*	41
Beginning of differentiation of posterior portion of pelvic girdle	37	39	42	36*	40	37*	40*	41
Complete contact between hypochord-postsacral elements	postmetamorph	46	46	—	46	—	46*	46
Almost complete hypochord ossification	postmetamorph	46	44	42	46	37–38*	46*	46
Beginning of chondrification of thid pair of postsacral elements	39	†	42	42	41	26	43	42
Position of joint hypochord-sacrourostyle at the end of Stage 46	posterior	posterior	anterior	posterior-44	anterior	—	posterior	posterior
Beginning of development lateral process first ppe	—	40	42	41*	43	—	†	—
Beginning of chondrification of sternum	42	43	42	42	42	†	42	42
Beginning of chondrification of omosternum	postmetamorph	43	—	—	postmetamorph	—	43	42
Beginning of ossification of isquium	postmetamorph	46	46	42	43	—	42	42
Contact of pectoral hemi-girdle	—	42*	41	42	42	—	42	42
Pubis: full contact of pelvic hemi-girdle	42	39	41	42	43	—	42	42
Ilial-sacrum contact	postmetamorph	45	44	42	43	—	46*	42
Foramen sacro-urostyle	46	46	†	†	†	—	46*	42
Beginning of expansion of sacral diapophyses	postmetamorph	44	42	42	postmetamoph	—	43	43
Femurs: perpendicular to axis of body	42	45	46	43	44	—	42	42
Anterior shape of ilium	curved	—	curved	pointed	pointed	—	curved	curved
Development of the ilium configuration (curved or pointed)	38	†	42	41	40	—	43	42
Ilium at level of presacral-sacrum joint	42	42	42	42	postmetamoph	—	46	45–46
Sesamoids	†	†	†	†	absents	—	46*	42

*The structure is evident at this stage, but earlier stages were not observed to confirm its presence in previous stages.
†Absent structure in the adult of this species.

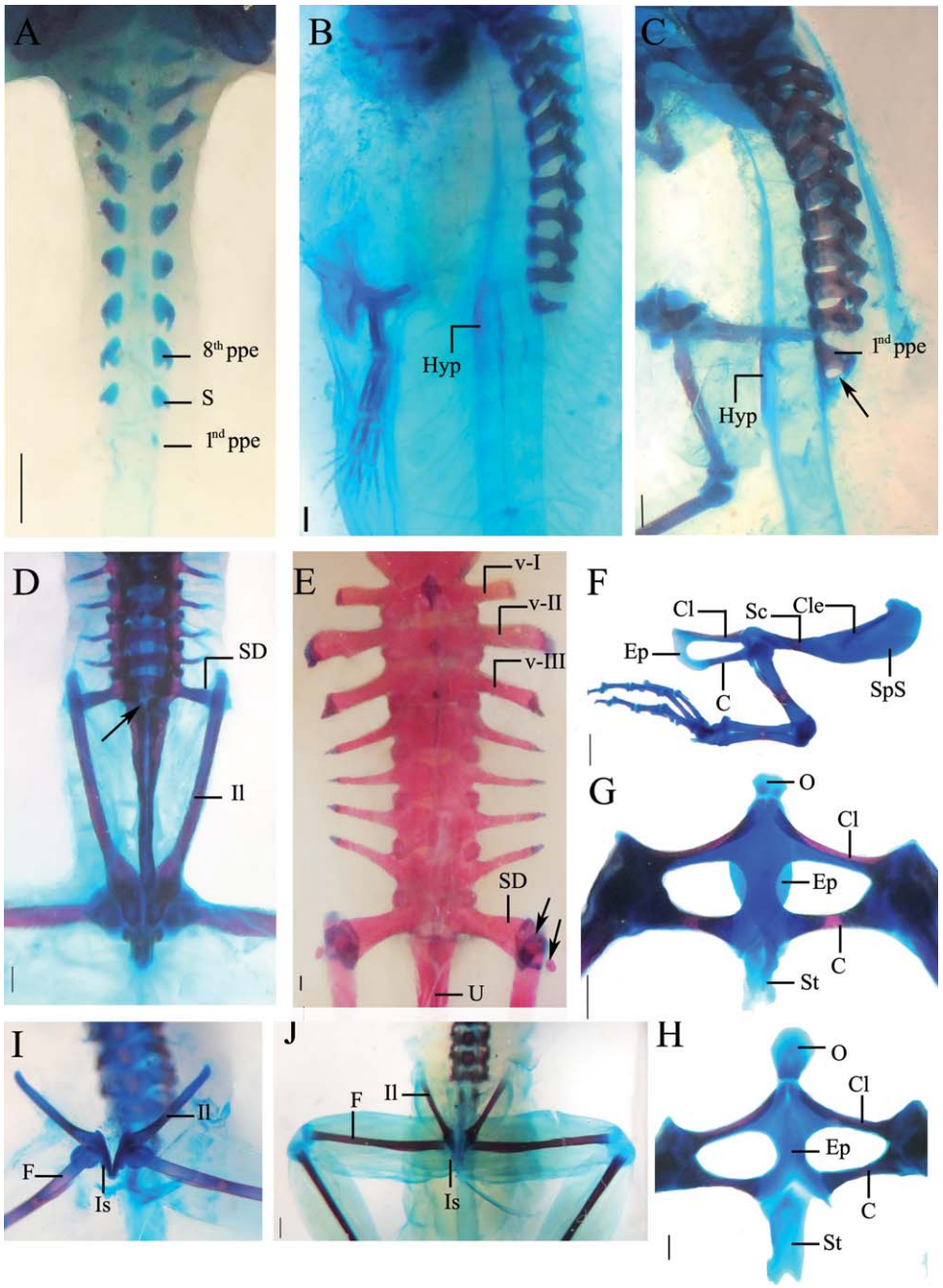

Fig. 1. *Scinax acuminatus*. **(A–E)** Vertebral column. A: Stage 29, in dorsal view. B: Stage 37, in lateral view. C: Stage 41, in lateral view, the spinal foramina is marked by black arrows. D: Stage 46, in dorsal view, the foramen between the sacrum and the postsacral elements is marked by one red arrow. E: adult in dorsal view, the sesamoids are marked by red arrows. **(F–H)** Pectoral girdle. F: Stage 41, hemigirdle, the anterior projection of the suprascapula is visible. G: Stage 43, in ventral view. H: Stage 46, in ventral view. **(I and J)** Pelvic girdle. I: Stage 41, in ventral view. J, Stage 42, in ventral view; C, coracoid; Cl, clavicle; Cle, Cleithrum; Ep, epicoracoid; F, femur; 1st ppe, first pair postsacral elements; 8th ppe, eighth pair presacral elements; Hyp, hypochord; Il, ilium; Is, Ischium; O, omosternum; S, sacrum; Sc, scapula; SD, sacral diapophyses; SpS, suprascapula; St, sternum; U, urostyle; v-I, vertebra I; v-II, vertebra II; v-III, vertebra III; Scale bars: 0.5 mm.

ossification (Fig. 2C), both pelvic hemigirdles contact each other at the level of ischium; the anterior projection of the suprascapula and the typical adult shape of the posterior region of the pelvic girdle are distinguishable; the anterior projection of the suprascapula and the typical adult shape of the posterior region of the pelvic girdle are distinguishable. The second pair of spinal foramina and the third pair of postsacral vertebra appear; the anterior end of ilium articulates with the sacral

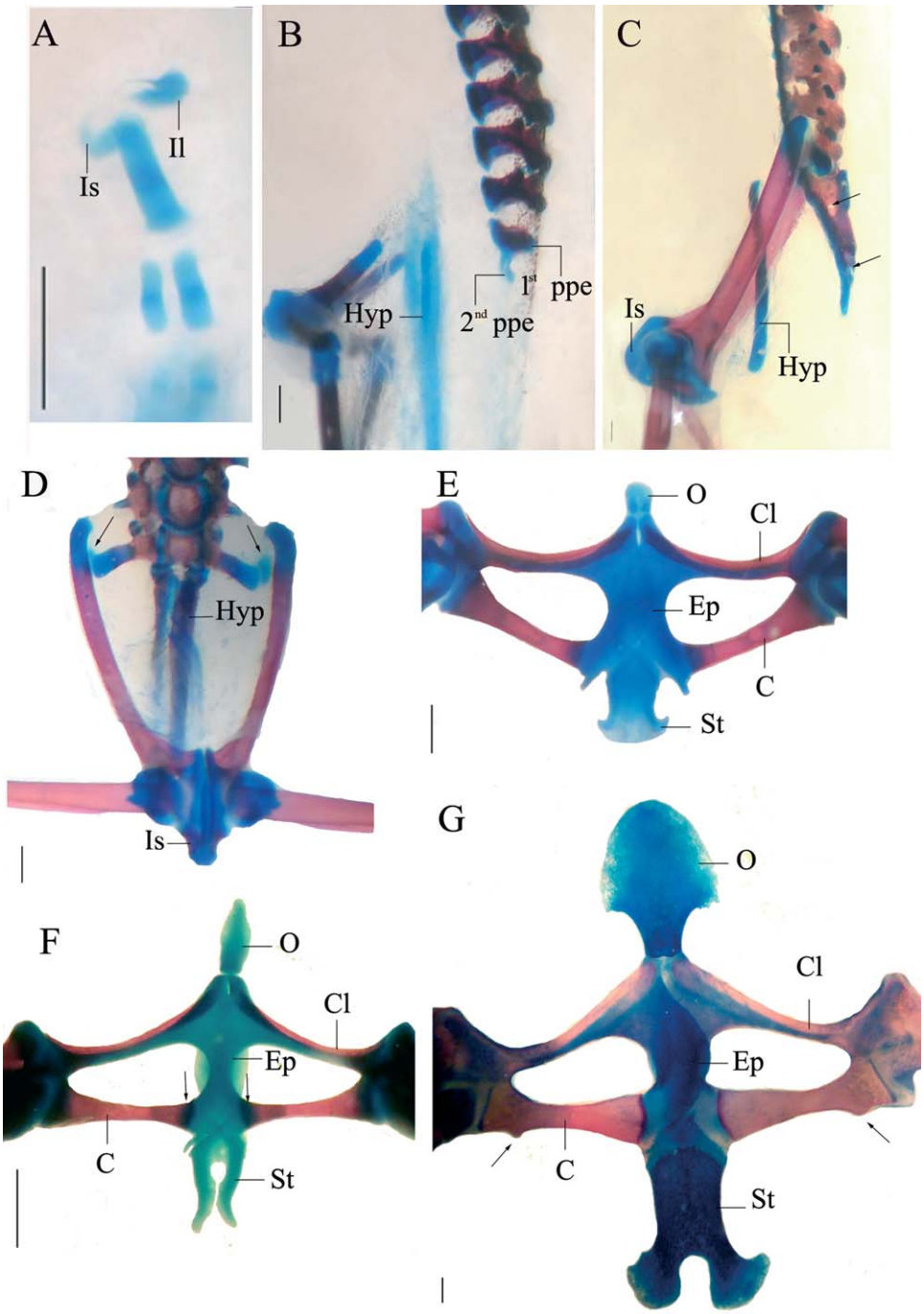

Fig. 2. *Scinax fuscovarius*. **(A and D)** Pelvic girdle. C: Stage 34, pelvic hemigirdle. D: Stages 42, in ventral view, the sesamoids are marked by black arrows. **(B and C)** Vertebral column. B: Stage 37, in lateral view. C: Stage 42, lateral view; the spinal foramina is marked by black arrows. **(E–G)** Pectoral girdle. E: Stage 42, in ventral view. F: Stage 46, in ventral view; the medial edges of the coracoids are marked by black arrows. G: Adult, in ventral view; coracoidal protuberance is marked by black arrows. C, coracoid; Cl, clavicle; Ep, epicoracoid; F, femur; 1st ppe, first pair postsacral elements; 2nd ppe, second pair postsacral elements; Hyp, hypochord; Il, ilium; Is, Ischium; O, omosternum; St, sternum; Scale bars: 0.5 mm.

diapophyses, and a cartilaginous sesamoid appears between both elements (Fig. 2D); the anterior end of the ilium reaches the anterior level of presacral vertebrae-sacrum articulation and a hole in the sacral region is formed (Fig. 2D), the omosternum and the epicoracoid horns begin development (Fig. 2E). Stages 43–44, the vertebral column and pectoral and pelvic girdles remain unchanged. Stage 46, the coracoids are already parallel to each other (Fig. 2F).

Adult. Vertebral column. The presence of neural spines shows intraspecific variation. The spines in presacral transverse processes are present. The longest transverse processes are those of the third and sacral vertebrae, whereas the shortest are those of the second vertebra (Fig. 1E). The sacral diapophyses are slightly expanded and posterolateraly directed (Fig. 1E). The posterior end of the urostyle reaches the pelvic girdle-limbs joint; the urostyle lacks transverse processes. The sacrum-urostyle articulation is bicondylar and a foramen between sacrum and urostyle is present. The vertebral column is shorter than the pelvic girdle. The transverse processes of the second, third, and sixth vertebrae are perpendicular to the axis of the column; in the fourth and fifth vertebrae, the processes are posteriorly oriented; and in the seventh and eighth, the processes are anteriorly oriented (Fig. 1E). The dorsal crest extends up to 57% of the urostyle length. Two sesamoids are present on the iliosacral region; the bigger one is cartilaginous and trapezoidal, the other one can be mineralized and round (Fig. 1E).

In *Scinax fuscovarius*, the transverse processes of the second, sixth, seventh, and eighth vertebrae are anteriorly oriented; the third vertebra is perpendicular to the axis of the column, and the fourth and fifth vertebrae are posteriorly oriented.

Pectoral girdle. The coracoids are longer than wide, with a protuberance in its antero-distal edges; they are perpendicular to the axis of body. The clavicles are slightly concave. The glenoid joint is synchondrotical. The scapula is distally expanded. The suprascapula shows an antero-distal projection; the antero-lateral edge of suprascapula is straight. There are instraspecific variations in the presence of an antero-lateral process in the sternum, which is present in FML28133 and FML28134, but is absent in FML28135. The sternum is not divided and lacks antero-lateral process; the left epicoracoid overlaps the right. In *S. fuscovarius*, the sternum is posteriorly divided (Fig. 2G), and the right epicoracoid overlaps the left (Fig. 2G).

Pelvic girdle. The ventral posterior region of the ilium is slightly expanded. The posterior edge of ischium shows a wide concavity. The ventrally concave pubis is completely calcified. The acetabular joint is cartilaginous.

Hypsiboas riojanus

Larval Ontogeny. At Stage 26, eight pairs of presacral vertebrae and a pair of sacral vertebrae are present. At Stage 27, the chondrification of the first pair of postsacral vertebrae begins. At Stage 31, the eight presacral and the sacral vertebrae are ossified; the first pair of postsacral vertebrae is cartilaginous (Fig. 3A). At Stage 33, the pectoral girdle begins to chondrify. At Stage 34, the first pair of postsacral vertebrae ossifies; the second pair of postsacral vertebrae appears. In the pectoral girdle, procoracoid, coracoid, and scapula are discernible (Fig. 3E). At Stage 35, the second pair of postsacral vertebrae and the ilium begin to ossify; the hypochord begins to chondrify; the sacral diapophyses and the suprascapula appear; the suprascapula chondrify (Fig. 3F). At Stage 36, epicoracoid begins to chondrify; scapula, clavicle, and cleithrum begin to ossify. At Stage 37, the third and fourth postsacral vertebrae begin to develop; the third one is visible as a cartilaginous projection from the second one; the fourth vertebra appears as a pair of cartilaginous structures (Fig. 3B). Both pelvic hemigirdles are closer at the level of the ischium, but they are still not in contact (Fig. 3L). The pelvic girdle begins to acquire the adult shape, which implies a postero-dorsal gap and a postero-ventrally rounded ilium. The posterior border of the ischium has a slightly pronounced groove. Coracoids begin to ossify (Fig. 3G). The suprascapula lacks antero-distal projection (Fig. 3G). The antero-lateral border of the suprascapula is straight. At Stage 38, the pair sheet of the presacral archs and those of the sacrum are ossified and fused; the hypochord begins to ossify; both pelvic hemigirdles contact at the level of ischium. The iliac shaft is at a 45° angle relative to the longitudinal axis of body. The antero-distal projection of the suprascapula appears. At Stage 39, the epicoracoid horns arches appear. At Stage 40, the ischium begins to ossify; both pelvic hemigirdles are closer to each other; the antero-lateral border of the suprascapula is rounded, and the antero-distal projection is visible (Fig. 3I). At Stage 41, the vertebral column and pelvic girdle remain unchanged. At Stage 42, the third pair of spinal foramina is present in the posterior end of the third pair of vertebrae; both pelvic hemigirdles are in full contact (Fig. 3M). The anterior end of the ilium reaches the level of the presacral vertebra; ilia are still not in contact with the sacral diapophyses; the sacro-urostyle joint forms (Fig. 3M). The sacral diapophyses are posteriorly oriented and the femurs are perpendicular to the longitudinal axis of the body. The sternum begins to develop as a chondrified and posteriorly bifurcate piece (Fig. 3H). At Stage 43, the vertebral column and girdle remain unchanged. At Stage 44, the hypochord exceeds the sacrum-urostyle joint anteriorly and the sacral diapophyses begin to ossify. At Stage 45, the only change is a greater development of the epicoracoid horns. At Stage 46, the hypochord is very close to the postsacral vertebrae (Fig. 3C); it is posterior at the level of the sacrum-urostyle joint. The sacral diapophyses maintain the posterior orientation. Two cartilaginous sesamoids are present between the iliosacral articulation (the presence of the elements is obvious in histological samples but not in diaphonized specimens).

Adult. Vertebral column. The neural spines are present in vertebrae I to IV (Fig. 3D). The

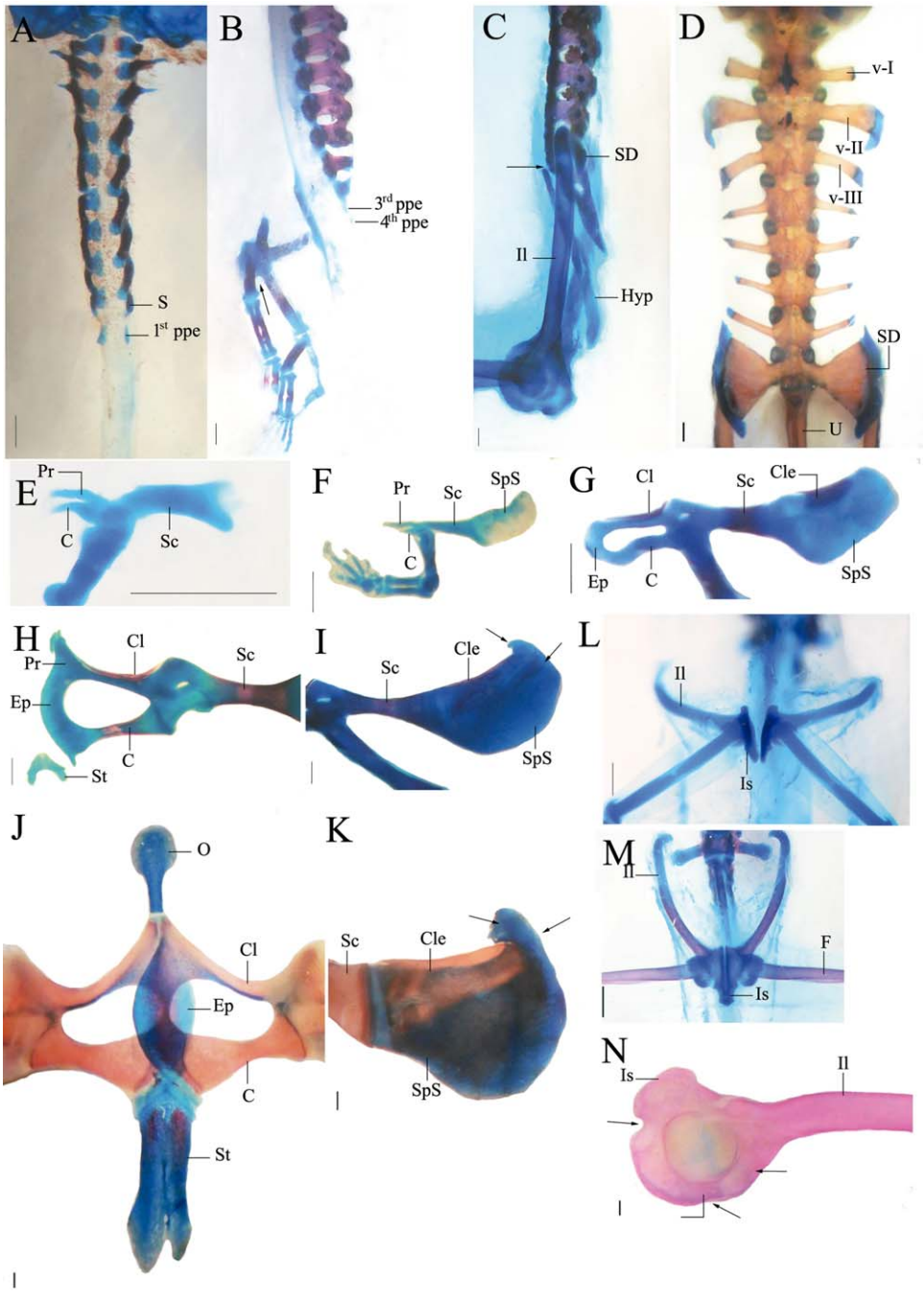

Fig. 3. *Hypsiboas riojanus*. Postcranial development. **(A–D)** Vertebral column and pelvic girdle. A: Stage 31, dorsal view. B: Stage 37, the arrow indicates the acetabular region of the pelvic girdle. C: Stage 46, lateral view; the arrow indicates the level reached by the anterior end of the hypochord. D: Adult, dorsal view. **(E–K)** Pectoral girdle. E: Stage 34. F: Stage 35. G: Stage 37. H: Stage 42, ventral view. I: Stage 40, dorsal view; arrows indicate anterior edge of suprascapula. J: Adult, ventral view. K: Adult, in dorsal view; arrows indicate the anterior edge of the suprascapula. **(L–N)** Pelvic girdle. L: Stage 37, ventral view. M: Stages 42, ventral view. N: Adult, lateral view; arrows indicate the borders of the acetabular region. C: coracoid. Cl, clavicle; Cle, cleithrum; Ep, epicoracoid; F, femur; 1st ppe, first pair postsacral elements; 3rd ppe, third pair postsacral elements; 4th ppe, fourth pair postsacral elements; Hyp, hypochord; Il, ilium; Is, Ischium; O, omosternum; Pr, procoracoid; S, sacrum; Sc, scapula; SD, sacral diapophyses; SpS, suprascapula; St, sternum; U, urostyle; v-I, vertebra I; v-II, vertebra II; v-III, vertebra III; Scale bars: 0.5 mm.

transverse processes lack spines. The longest transverse processes are the sacral, and the shortest are those of the second vertebra. The transverse processes of the second, sixth, seventh, and eighth vertebrae are anteriorly oriented; the transverse processes of the third vertebra are

perpendicular to the axis of the column; and those of the fourth and fifth vertebrae are posterior (Fig. 3D). The sacral diapophyses are greatly expanded and anteriorly oriented. The posterior end of the urostyle reaches the pelvic girdle-limb joint. The urostyle lacks transverse processes; the dorsal crest extends up to 71% of its length. The sacrum-urostyle articulation is bicondylar and lacks foramen. The vertebral column is shorter than the pelvic girdle. A sesamoid is present at the iliosacral articulation.

Pectoral girdle. A protuberance is be present in the coracoids. The coracoids are longer than wide; they are diagonal, with the distal end anteriorly oriented (Fig. 3J). The clavicles are anteriorly slightly concave. The glenoid joint is synchondrotic. The scapula is distally expanded. The suprascapula has an antero-distal projection and rounded antero-lateral edge (Fig. 3K). The left epicoracoid overlaps the right epicoracoid (Fig. 3J). The sternum is posteriorly divided and shows antero-lateral processes (Fig. 3J).

Pelvic girdle. The angle between the iliac shaft and the anterior edge of the acetabulum is right or obtuse. The ischium shows a narrow concavity (Fig. 3N). The acetabular joint varies intraspecifically: it is either synchondrotic and synostotic or completely fused. The pubis is concave ventrally (Fig. 3N). The degree of ossification of the pubis is variable: cartilaginous with mineralization or entirely mineralized/calcified.

Phyllomedusa Species

The description of the ontogenic and adult pattern is based on *Phyllomedusa sauvagii*, with reference to the characters that are different in *P. azurea* and *P. boliviana*.

Larval Ontogeny. At Stage 33, eight presacral vertebrae, one sacral and one postsacral vertebrae are present. At Stage 34, chondrification of girdle, limb, scapula, procoracoid, and ilium-ischium begins (Fig. 4J). At Stage 35, chondrification of the coracoid and suprascapula and ossification of the scapula starts (Fig. 4D). At Stage 36, the sacral and a pair of presacral vertebrae are ossified. At Stage 37, chondrification of the hypochord and second pair of postsacral vertebrae and the development of sacral dispophyses occurs (Fig. 4A); and ossification of the clavicle and cleithrum begins (Fig. 4E). Between Stages 38 and 39, the vertebral column and girdle remain unchanged. At Stage 40, both pelvic hemigirdles are in contact at the level of the ischium and ossification of the sacral diapophyses begins; ossification of the coracoid begins (Fig. 4F). At Stage 41, the first pair of spinal foramina is formed; the third pair of postsacral vertebrae begins to develop as a cartilaginous projection from the second one; the hypochord begins to ossify, and both pectoral and pelvic girdles remain unchanged from Stage 40 onward. At Stage 42, the sternum begins to develop; the epicoracoid horn begins to develop (Fig. 4G). At Stage 43, chondrification of the third pair of postsacral vertebrae begins, the sacral diapophyses begin to expand, the lateral processes in the first pair of postsacral vertebrae begins to develop, and the pelvic girdle shows the adult shape. The contact between ilium and sacral diapophysis occurs. The third pair of spinal foramina is formed, both femurs are already perpendicular to the axis of the body and pectoral girdle remains unchanged. At Stage 45, the vertebral column and pelvic girdle remain unchanged. At Stage 46, the contact between hypochord and postsacral vertebrae is completed and the anterior end of the hypochord exceeds the level of the anterior end of the first pair of postsacral vertebrae (Fig. 4B); the sacral diapophyses begin to expand (Fig. 4K).

Variation to the pattern described above, in *Phyllomedusa azurea* and *P. boliviana*, are: at Stage 36, chondrification of the hypochord and suprascapula and ossification of scapula and first pair of postsacral vertebrae are evident (Figs. 5A,F and 6A,D). At Stage 42, chondrification of the third pair of postsacral vertebrae begins (Figs. 5C and 6B), the sacral diapophyses begin to expand, the lateral processes in the first pair of postsacral vertebrae begins to develop (Figs. 5D and 6C), and the pelvic girdle shows the adult shape.

Other variations in *Phyllomedusa azurea* are: At Stage 31, eight presacral, one sacral and one postsacral vertebra are present. At Stage 38, ossification of the clavicle and cleithrum begins. At Stage 39, chondrification of the second pair of postsacral vertebrae and hypochord occurs (Fig. 5B); the coracoids begin to ossify (Fig. 5G). At Stage 41, contact between both hemipelvic girdles is completed. At Stage 43, the third pair of spinal foramina is formed in the posterior end of the third pair of postsacral vertebrae; the third pair of postsacral vertebrae disappears, and both pectoral and pelvic girdles remain unchanged. At Stage 46, both femurs are already perpendicular to the axis of the body and the ischium begins to ossify.

Variation to the developmental pattern in *Phyllomedusa boliviana* are: At Stage 36, the ossification of the second postsacral vertebrae, hypochord, scapula, clavicle, and cleithrum is present. At Stage 41, both pelvic hemigirdles contact at the level of the ischium and ossification of the sacral diapophyses begins. At Stage 43, the vertebral column and girdles remain unchanged; the development of the epicoracoid horn begins; the vertebral column and pelvic girdle remains unchanged, and the suprascapula shows an anterior projection (Fig. 5H).

Adult. Vertebral column. The presence of the neural spines varies between vertebrae. The transverse processes of the third and sacral vertebrae are the longest, and those of the second and

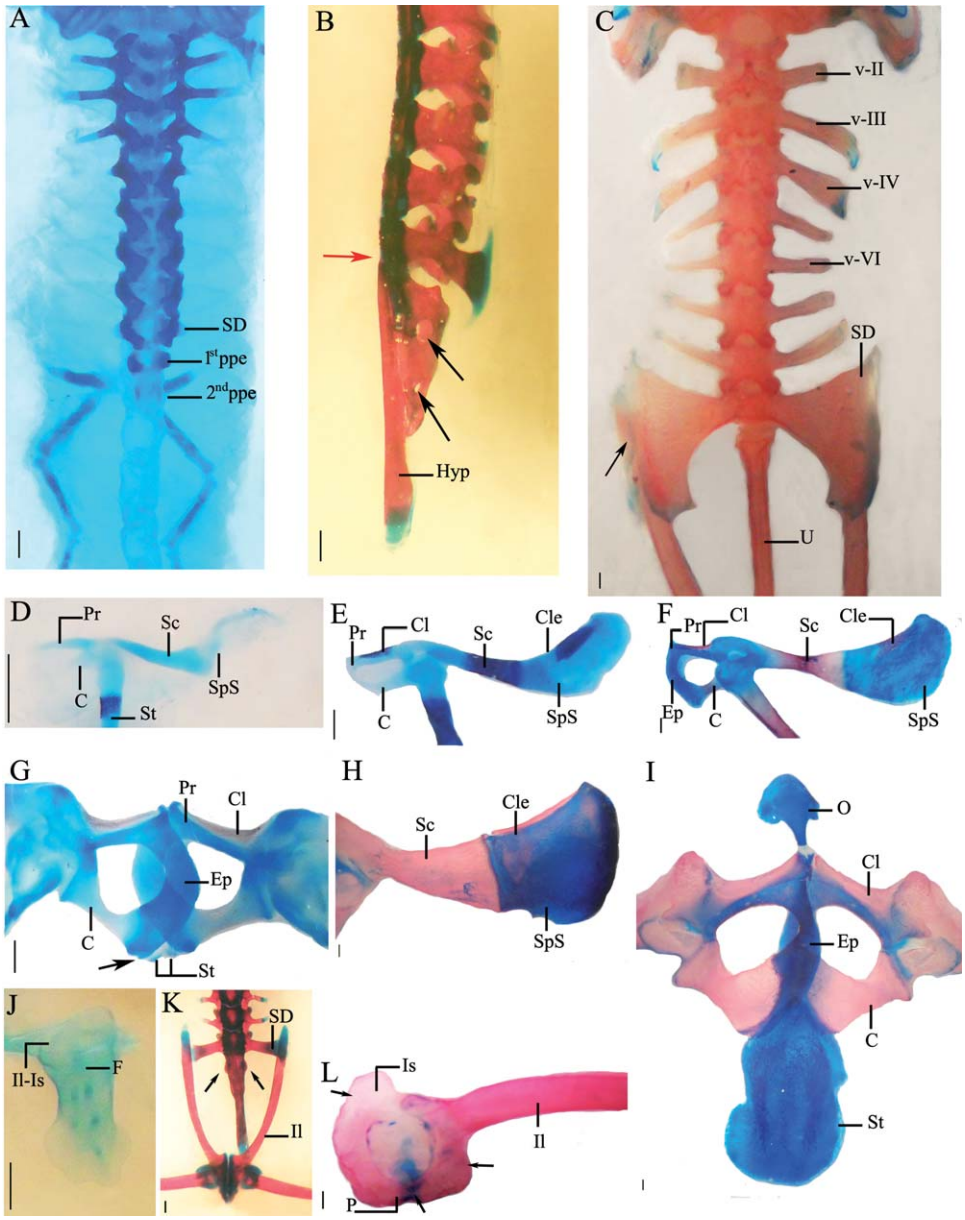

Fig. 4. *Phyllomedusa sauvagii*. **(A–C)** Vertebral column and pelvic girdle. A: Stage 37, dorsal view. B: Stage 46, lateral view; the vertebral column is disarticulated from the pelvic girdle; the red arrow indicates the level that reaches the anterior end of the hypochorda, and the black arrows indicate the spinal foramina. C: Adult, dorsal view; the arrow indicates sesamoids. **(D–I)** Pectoral girdle. D: Stage 35. E: Stage 37. F: Stage 40. G: Stage 42, ventral view; the arrow indicates epicoracoid horns. H: Adult, ventral view; I: Adult, dorsal view, arrows indicate the anterior edge of the suprascapula. **(J–L)** Pelvic girdle. J: Stage 34. S: Stage 36. K: Stages 46, ventral view, arrows indicate the lateral process of the first pair of postsacral elements. L: Adult, lateral view; arrows indicate the borders of the acetabular region. C, coracoid; Cl, clavicle; Cle, cleithrum; Ep, epicoracoid; F, femur; 1st ppe, first pair postsacral elements; 2nd ppe, second pair postsacral elements; Hyp, hypochord; Il, ilium; Is, Ischium; O, omosternum; P, pubis; Pr, procoracoid; Sc, scapula; SD, sacral diapophyses; SpS, suprascapula; St, sternum; U, urostyle; v-II, vertebra II; v-III, vertebra III; v-VI, vertebra VI. Scale bars: 0.5 mm.

seventh vertebrae are the shortest (Fig. 4C). The sacral diapophyses are moderately expanded and anteriorly directed. The anterior end of the urostyle has spine-shaped lateral processes. The posterior end of the urostyle reaches the pelvic girdle-limbs joint. The dorsal crest extends up to 65% of the length of urostyle. The sacrum-urostyle articulation is monocondylar. The vertebral column is shorter than the pelvic girdle. Two oval sesamoids—one clearly longer than the other—are present on the iliosacral articulation.

Variations to the adult vertebral column pattern described above, in *Phyllomedusa azurea* and *P. boliviana*, are: the sacral dispophyses are greatly expanded; the position of the posterior end of the urostyle relative to the pelvic girdle joint varies

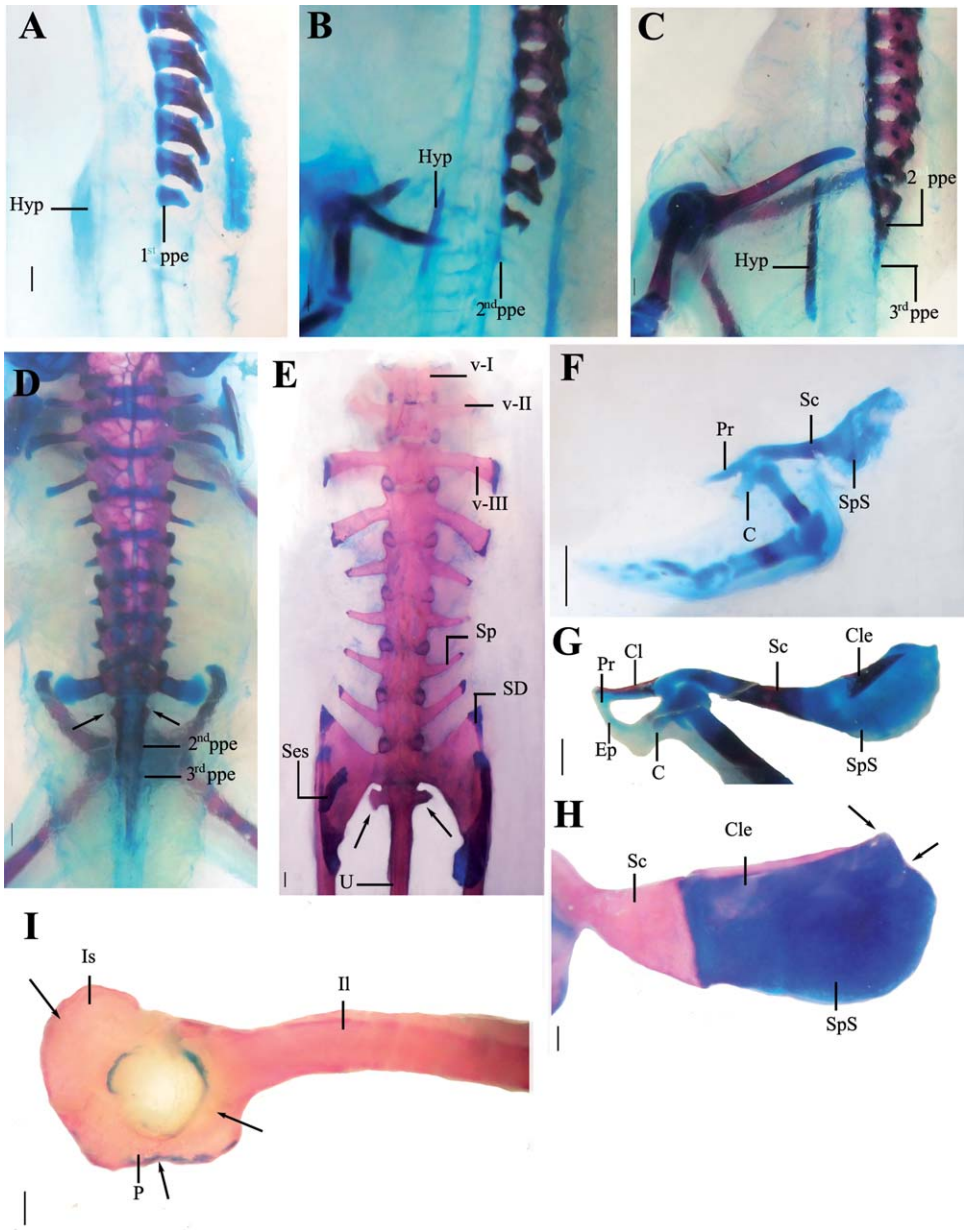

Fig. 5. *Phyllomedusa azurea*. **(A–E)** Vertebral column. A: Stage 36, lateral view. B: Stage 39, lateral view. C: Stage 42, lateral view. D: Stage 42, dorsal view; arrows indicate the lateral processes of the first pair postsacral elements. E: Adult, dorsal view; arrows indicate the transverses process of the urostyle. **(F–H)** Pectoral girdle. F: Stage 36. G: Stage 39. H: Adult, dorsal view; arrows indicate the anterior edge of the suprascapula. **(I)** Pelvic girdle, adult lateral view; the arrow indicates the borders of the acetabular region. C: coracoid. Cl: clavicle. Cle: cleithrum. Ep: epicoracoid. 1st ppe: first pair postsacral elements. 2nd ppe: second pair postsacral elements. 3rd ppe: third pair postsacral elements. Hyp: hypochord. Il: ilium. Is: Ischium. P: pubis. Pr: procoracoid. Sc: scapula. SD: sacral diapophyses. Ses: sesamoid. Sp: spine of the presacral transverse process. SpS: suprascapula. v-I: vertebra I. v-II: vertebra II. v-III: vertebra III. Scale bars: 0.5 mm.

intraspecifically in both species; one cartilaginous sacral sesamoid is present. Further, in *P. azurea* the transverse processes of second and sixth vertebrae are the shortest; the anterior end of the urostyle has lateral processes as elongated projections (Fig. 5E); the dorsal crest of the urostyle extends up to 50% of the length of the urostyle; the vertebral column is longer than the pelvic girdle. In *P. boliviana*, the transverse processes of second vertebrae are the shortest; the dorsal crest of the urostyle extends up to 84% of the length; the length of vertebral column relative to the pelvic girdle varies intraspecifically.

Pectoral girdle. The coracoid lies diagonally and its length is twice its width or shorter (Fig. 4I). The glenoid joint is synchondrotic. The sternum is

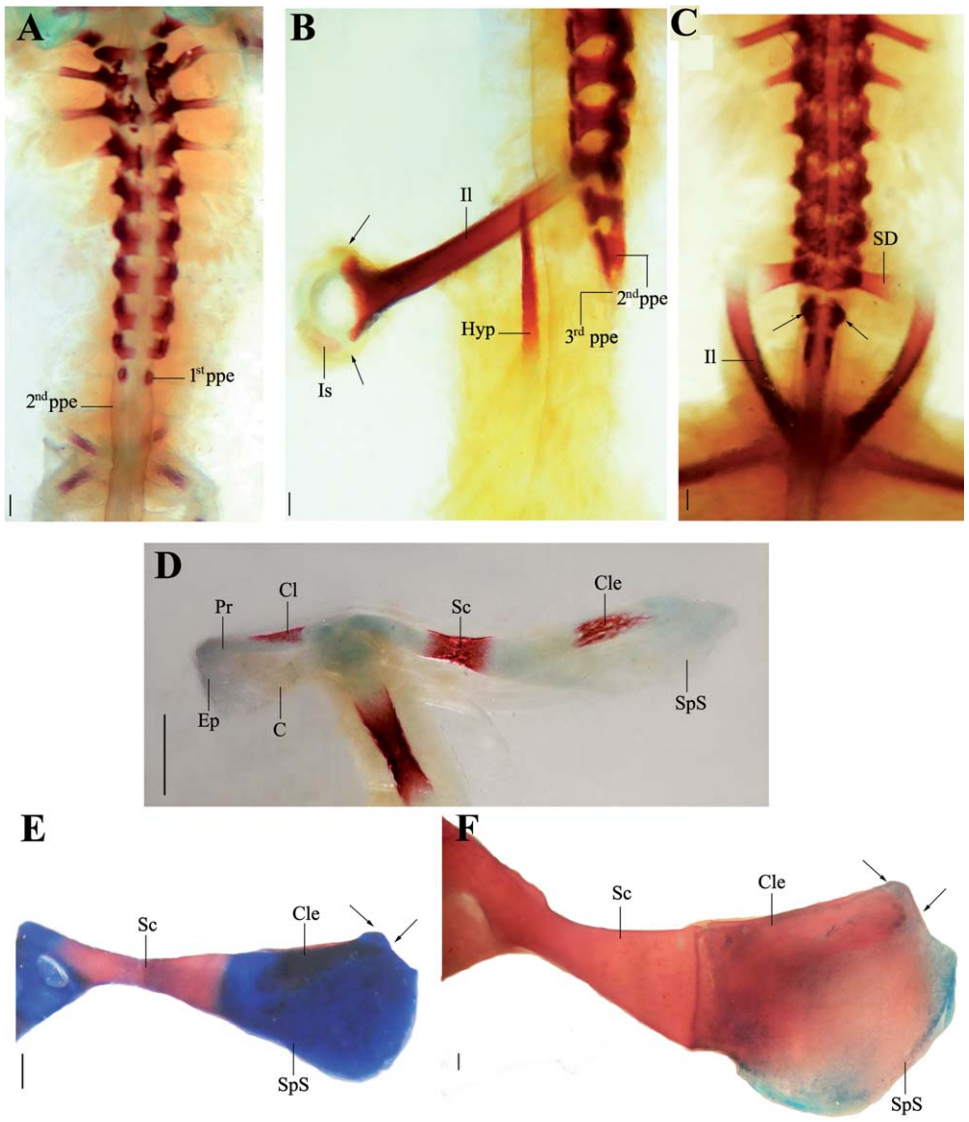

Fig. 6. *Phyllomedusa boliviana*. **(A–C)** Vertebral column. A: Stage 36, in dorsal view. B: Stage 42, in lateral view, the differentiation of the acetabular region is marked by black arrows. C: Stage 42 in dorsal view, the lateral process of the first pair of postsacral elements is indicated with black arrows. **(D–F)** Pectoral girdle. D: Stage 36, hemigirdle; the anterior edge of the suprascapula is indicated with a black arrow. E: Stage 43, in dorsal view, the anterior edge of the suprascapula is indicated with black arrows. F: Adult, in dorsal view, the anterior edge of the suprascapula is indicated with red arrows. C: coracoid. Cl, clavicle; Cle, Cleithrum; Ep, epicoracoid; 1st ppe, first pair postsacral elements; 2nd ppe, second pair of postsacral elements; 3rd ppe, third pair of postsacral elements; Hyp, hypochord; Il, ilium; Is, Ischium; Pr, procoracoid; Sc, scapula; SD, sacral diapophyses; SpS, suprascapula. Scale bars: 0.5 mm.

a single element and lacks the antero-lateral processes (Fig. 4I); the scapula is moderately expanded. The suprascapula lacks the anterior projection (Fig. 4H). The right epicoracoid overlaps the left one (Fig. 4I).

Variations to the pattern described above are: In *Phyllomedusa azurea* and *P. boliviana*, the scapula is greatly expanded; the antero-distal edge of the suprascapula is concave (Figs. 5H and 6F). In *P. azurea*, the presence of the antero-lateral processes of the sternum varies. Some specimens of *P. boliviana* present coracoids with postero-distal protuberances. Also, in this species; the clavicles are concave in the distal region, and the glenoid joint can be synchondrotic or synostotic.

Pelvic girdle. The angle between the ilial shaft and the border of the anterior acetabular plate is almost straight. The postero-dorsal edge of the ischium is rounded (Figs. 4L). The acetabular joint is synostotic (Fig. 4L). The pubis can be cartilaginous with mineralization. A variation observed, in *Phyllomedusa azurea* and *P. boliviana*, is a synostotic acetabular joint. Besides, *P. azurea* show a ventral slit in the pubis (Fig. 5I).

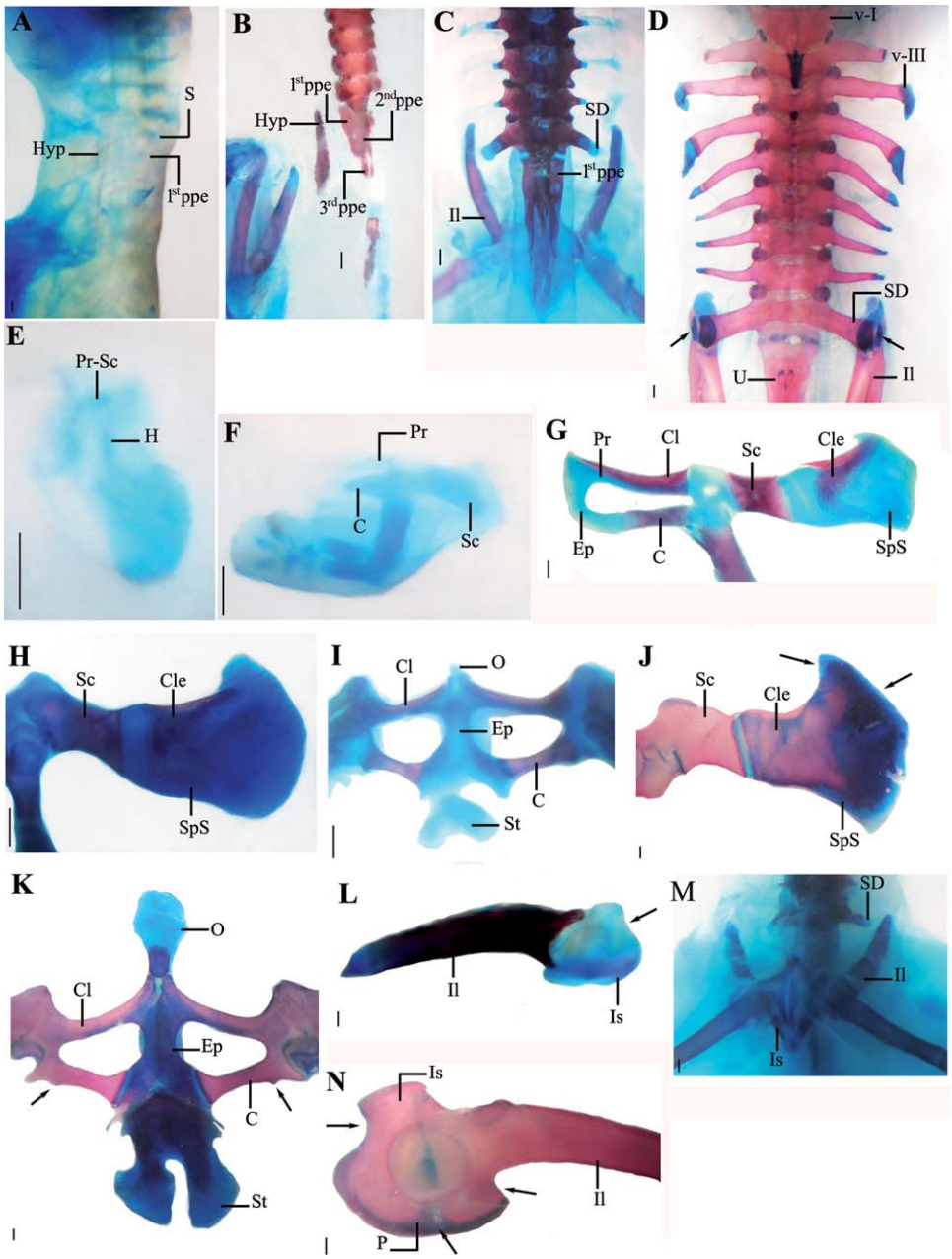

Fig. 7. *Pseudis platensis*. (**A–D**) Vertebral column. A: Stage 31 – 34, in lateral view. B: Stage 37 – 38, in lateral view, the spinal foramina is indicated with a black arrow. C: Stage 43, in dorsal view. D: Adult, in dorsal view, the sesamoids are indicated with black arrows. **(E–K)** Pectoral girdle. E: Stage 31 – 34, hemigirdle. F: Stage 34 – 37, hemi-girdle. G: Stage 37 – 38, hemi-girdle. H: Stage 43, in dorsal view. I: Stage 43, in ventral view; the epicoracoid horns are indicated with black arrows. J: Adult in dorsal view; the anterior edge of the suprascapula is indicated with black arrows. K: Adult in ventral view; the coracoid protuberances are indicated with black arrows. **(L–N)** Pelvic girdle. L: Stage 37 – 38, hemi-girdle in lateral view; the groove of the ischium is indicated with black arrow. M: Stage 43, in ventral view. N: Adult, in lateral view of the acetabular region. C, coracoid; Cl, clavicle; Cle, Cleithrum; Ep, epicoracoid; 1st ppe, first pair of postsacral elements; 2nd ppe, second pair of postsacral elements; 3rd ppe, third pair of postsacral elements; Hyp, hypochord; Il, ilium; Is, ischium; O, omosternum; P, pubis; Pr, procoracoid; S, sacrum; Sc, scapula; SD, sacral diapophyses; SpS, suprascapula; St, sternum; U, urostyle; v-I, vertebra I; v-III, vertebra III. Scale bars: 0.5 mm.

Pseudis platensis

Larval Ontogeny. At Stage 26, eight pairs of presacral vertebrae and one pair of sacral vertebrae are observed. At Stage 28, the first pair of postsacral vertebrae and the hypochord are present. Between Stages 31 and 34, the eight presacral vertebra, the sacral vertebra and hypochord are ossified (Fig. 7A); the girdles and limbs begin to develop (Fig. 7E). Between Stages 35 and 37, the vertebral column remains unchanged, and procoracoids, coracoids and scapulae are differentiated

(Fig. 7F). At Stages 37 and 38, ossification of three pairs of postsacral vertebrae, hypochord, coracoids, scapula, clavicle and cleithrum occurs (Fig. 7B,G); the suprascapula shows an antero-distal projection (Fig. 7G); the posterior border of the ischium has a slightly pronounced groove (Fig. 7L). At Stage 43, the sacral diapophyses are developed (Fig. 7C); both pelvic hemigirdles are in full contact (Fig. 7M); the ischium is ossified; the omosternum, sternum and epicoracoid horns are present (Fig. 7I); the coracoid has a bump on its posterior distal edge (Fig. 7H).

Adult. Vertebral column. The neural spines are present in vertebrae I to III. The presence of the spines in presacral transverse processes varies (Fig. 7D). The third and fourth transverse processes are longer than the others (Fig. 7D). The second and the sacral transverse processes are the shortest (Fig. 7D). The sacral diapophyses are not expanded and are posterolaterally directed. The transverse processes of the seventh and eighth vertebrae are antero-laterally oriented. The second and third transverse processes are perpendicular to the axis of the column, whereas the fourth, fifth and sixth transverse processes are posterolaterally oriented (Fig. 7D). The posterior end of the urostyle reaches the pelvic girdle-limbs joint. The dorsal crest extends up to 74% of the urostyle length. The urostyle has protuberant paired lateral processes. The sacro-urostyle articulation is bicondylar and with a foramen present (Fig.7I). The vertebral column is shorter than the pelvic girdle (supporting information Appendix II). A cartilaginous sesamoid is present on the iliosacral articulation (Fig. 7D).

Pectoral girdle. The coracoid length is less than or equal to twice its width. The coracoid protuberance is present. The coracoids are diagonal relative to the axis of the body (Fig. 7K). The clavicle shows a broad concavity. The scapula is not expanded. The suprascapula has distal anterior projection; its distal anterior edge is convex (Fig. 7J). The sternum is posteriorly divided and shows antero-lateral processes (Fig. 7K). The glenoid joint is synchondrotic. The left epicoracoid overlaps the right one (Fig. 7K).

Pelvic girdle. The angle between the ilial shaft and anterior edge of the acetabular plate is acute. The posterior edge of the ischium shows a broad concavity (Fig. 7N). The pubis is cartilaginous and lacks a ventral groove. The acetabular joint is synchondrotic (Fig. 7N).

Lysapsus limellum

Larval Ontogeny. At Stage 26, eight pairs of presacral vertebrae are present. Between Stages 27 and 31, the pair of sacral vertebrae is present. At Stage 33, the first pair of postsacral vertebrae (Fig. 8A) and sketches of girdles and limbs are present. At Stage 35, the chondrification of the hypochord and suprascapula begins (Fig. 8B,F). At Stage 36, the ossification of the eighth pair of presacral vertebrae and sacral vertebra begins. At Stage 39, both pelvic hemigirdles are in contact. The second pair of postsacral vertebrae begins to develop as cartilaginous projections from the first pair of postsacral vertebrae (Fig. 8C). The first and second pairs of spinal foramina are formed (Fig. 8C). The sacral diapophyses, epicoracoid horns, and coracoid protuberances begin to develop (Fig. 8G); coracoids, clavicle and cleithrum begin to ossify (Fig. 8J). The antero-distal edge of the suprascapula is concave and the anterior projection is visible (Fig. 8G). At Stage 40, the first pair of postsacral vertebrae and the hypochord begin to ossify (Fig. 8D); the lateral processes of the first pair of postsacral vertebrae begin to develop (Fig. 8D). At Stage 43, the omosternum and the sternum begin to develop (Fig. 8H); both hemigirdles are in full contact. At Stage 44, the anterior end of the ilium reaches the level of the eighth presacral vertebra; the sacral diapophyses begin to expand. At Stage 45, the anterior ends of the ilia articulate with the sacral diapophyses; both femurs are already perpendicular to the axis of the body; the anterior end of the hypochord and postsacral vertebrae are in contact; only the first pair of spinal foramina is present. At Stage 46, the contact between hypochord and postsacral vertebrae is completed and they become fused; the anterior end of the hypochord does not exceed the level of the anterior end of the first pair of postsacral vertebrae; the ischium begins to ossify.

Adult. Vertebral column. Neural spines are present in vertebrae I and II. The spines in presacral transverse process are absent (Fig. 8E). The third and fourth transverse processes are longer than the others. The second and eighth transverse processes are the shortest (Fig. 8E). The sacral diapophyses are slightly expanded and posteriorly directed. The transverse processes of the second, third, seventh, and eighth vertebrae are antero-laterally oriented. The transverse process of the fourth, fifth, and sixth vertebrae are posterolaterally oriented (Fig. 8E). The posterior end of the urostyle reaches the pelvic girdle-limbs joint. The dorsal crest extends up to 50% the length of urostyle. The urostyle has protuberant lateral processes (Fig. 8E). The sacro-urostyle articulation is bicondylar, with a foramen present. The vertebral column is shorter than the pelvic girdle. A calcified sesamoid is present on the ilio-sacral articulation (Fig. 8E).

Pectoral girdle. The coracoids are longer than wide; they are diagonal, with the distal end anteriorly oriented in relation to the axis of the body (Fig. 8I). The coracoid protuberance is present (Fig. 8I). The clavicle is slightly concave (Appendix II). The scapula is distally expanded. The suprascapula has distal anterior projection; its edge is concave (Fig. 8J). The sternum is posteriorly

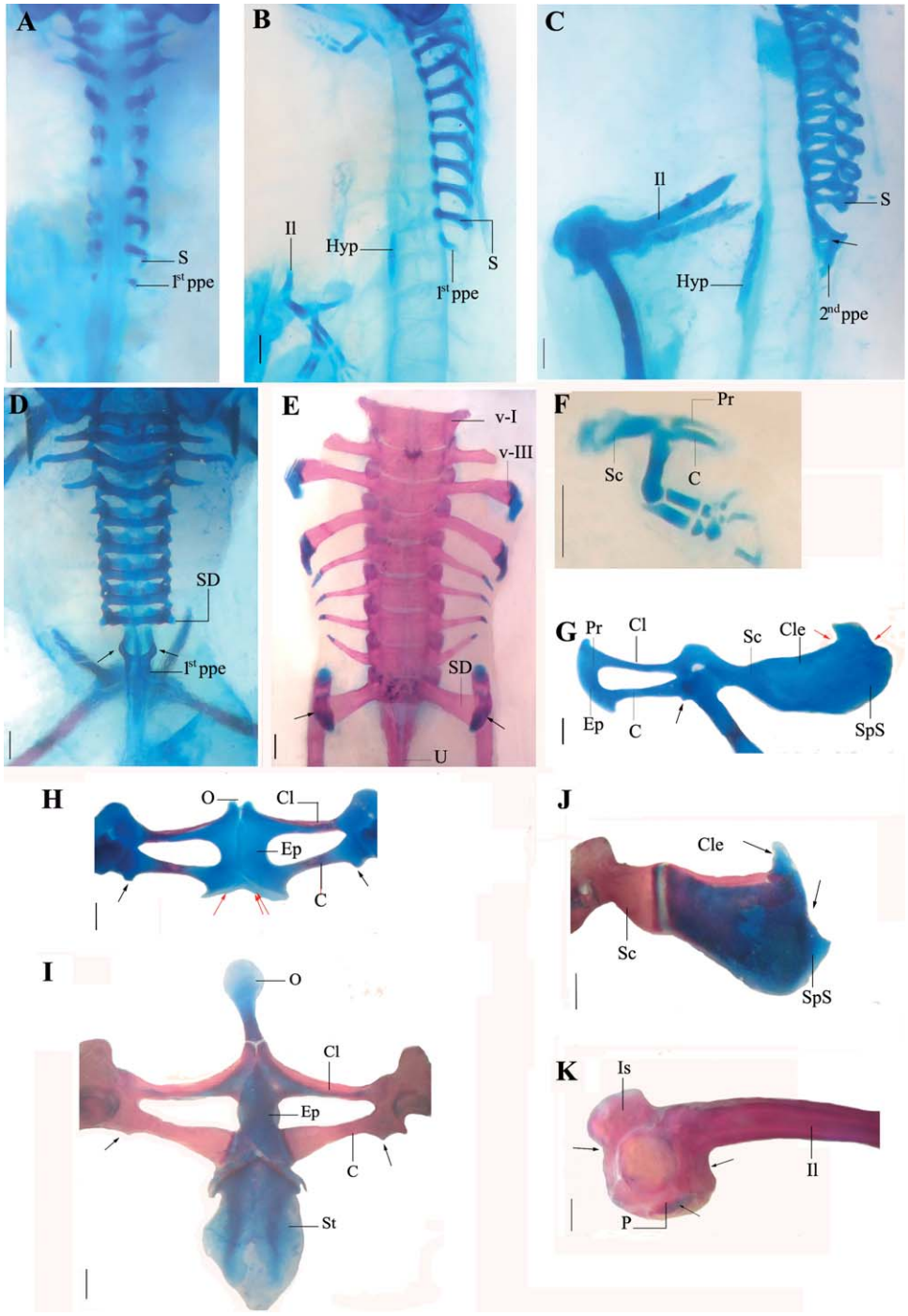

Fig. 8. *Lysapsus limellum*. (**A–E)** Vertebral column. **A**: Stage 33, in dorsal view. **B**: Stage 35, in lateral view. **C**: Stage 39, in lateral view; the differentiation of the acetabular region is indicated with black arrows. **D**: Stage 40, in dorsal view; the lateral process of the first pair the postsacral of elements are indicated with black arrows. **E**: Adult, in dorsal view; the sesamoids are indicated with a red arrow. **(F to J)** Pectoral girdle. **F**: Stage 35, hemi-girdle. **G**: Stage 39, hemi-girdle; the anterior edge of the suprascapula is indicated with red arrows. **H**: Stage 43, in ventral view; the sterna sketch is indicated with red arrows. **I**: Adult, in ventral view; the coracoid protuberances are indicated with black arrows. **J**: Adult, in dorsal view; the anterior edge of the suprascapula is indicated with black arrows. **(K)** Pelvic girdle, adult in lateral view of the acetabular region. C, coracoid; Cl, clavicle; Cle, cleithrum; Ep, epicoracoid; 1st ppe, first pair of postsacral elements; 2nd ppe, second pair of postsacral elements; Hyp, hypochord; Il, ilium; Is, Ischium; O, omosternum; P, pubis; Pr, procoracoid; S, sacrum; Sc, scapula; SD, sacral diapophyses; SpS, suprascapula; St, sternum; U, urostyle; v-I, vertebra I; v-III, vertebra III. Scale bars: 0.5 mm.

divided; it has an antero-lateral process (Fig. 8I). The glenoid joint is synostotic. The right epicoracoid overlaps the left one (Fig. 8I).

Pelvic girdle. The angle between the ilial shaft and anterior the border of the acetabular plate is acute. The postero-dorsal edge of the ischium has a broad concavity (Fig. 8K). The pubis is cartilaginous and lacks a ventral groove. The elements of the acetabulum are fused (Fig. 8K).

Phylogenetic mapping. The variation observed can be summarized in 68 characters, including 28 of larval osteology, 35 of adult osteology and five histological characters, which are listed below. The state "beginning of ossification" in several characters refers to when elements become visible based on alcian blue staining; although, employing other stains could reveal an earlier development.

1. Beginning of chondrification of the eight pair of presacral vertebrae: (0) Larval I, (1) Larval II, (2) Larval III.
2. Beginning of chondrification of the sacrum: (0) Larval I, (1) Larval II, (2) Larval III.
3. Beginning of chondrification of the first pair of postsacral vertebrae: (0) Larval I, (1) Larval II, (2) Larval III.
4. Beginning of chondrification of the girdles and limbs: (0) Larval I, (1) Larval II, (2) Larval III.
5. Beginning of chondrification of the second pair of postsacral vertebrae: (0) Larval III, (1) Larval IV.
6. Beginning of chondrification of the hypochord: (0) Larval I, (1) Larval II, (2) Larval III, (3) Larval IV.
7. Beginning of ossification of the first pair of postsacral vertebrae: (0) Larval III, (1) Larval IV.
8. Beginning of ossification of the coracoids: (0) Larval III, (1) Larval IV.
9. Beginning of ossification of the scapulae: (0) Larval III, (1) Larval IV.
10. Beginning of ossification of the second pair of postsacral vertebrae: (0) Larval III, (1) Larval IV, (2) Early metamorphic.
11. Beginning of ossification of the hypochord: (0) Larval I, (1) Larval II, (2) Larval III, (3) Larval IV.
12. Beginning of ossification of the clavicles and cleithra: (0) Larval III, (1) Larval IV.
13. Beginning of development of the sacral diapophyses: (0) Larval III, (1) Larval IV.
14. Beginning of differentiation of the suprascapulae: (0) Larval III, (1) Larval IV, (2) Early metamorphic.
15. Beginning of differentiation of acetabular area (pubis, ischium and part of the ilium) of pelvic girdle: (0) Larval III, (1) Larval IV, (2) Early metamorphic.
16. Complete contact between hypochord-postsacral vertebrae: (0) Late metamorphic, (1) Does not happen until late in metamorphosis.
17. Almost complete (approximately 90%) hypochord ossification: (0) Larval III, (1) Larval IV, (2) Early metamorphic, (3) Late metamorphic, (4) Does not happen until late in metamorphosis.
18. Beginning of chondrification of third pair of postsacral vertebrae: (0) Larval III, (1) Larval IV, (2) Early metamorphic.
19. Position of hypochord-sacro-urostyle joint at the end of Stage 46: (0) Posterior, (1) Anterior.
20. Visibility of the first pair of postsacral vertebrae with alcian blue staining: (0) Larval IV, (1) Early metamorphic.
21. Beginning of chondrification of omosternum: (0) Early metamorphic, (1) Late metamorphic.
22. Beginning of ossification of ischium: (0) Larval IV, (1) Early metamorphic, (2) Late metamorphic.
23. Contact along the middle line of pectoral hemigirdles: (0) Larval IV, (1) Early metamorphic.
24. Pubis: full contact of pelvic hemigirdles, (1) Early metamorphic, (2) Late metamorphic.
25. Ilio-sacrum contact: (0) Early metamorphic, (1) Stages 45 to 46.
26. Beginning of formation of bicondylar joint: (0) Early metamorphic, (1) Late metamorphic.
27. Beginning of expansion of sacral diapophyses: (0) Early metamorphic, (1) Late metamorphic.
28. Femurs: perpendicular to axis of body: (0) Larval IV, (1) Early metamorphic, (2) Late metamorphic.
29. Shape of the anterior end of ilium. Through the development the shape may change. This variation does not correspond with the adult configurations, which is more conservative. The different shapes of the anterior end of the ilium observed in the larval stages are: (0) Rounded, (1) Pointed, (2) Straight.
30. Development of the ilial configuration (curved or pointed): (0) Larval IV, (1) Early metamorphic.
31. Sesamoid in the iliosacral region: (0) Early metamorphic, (1) Late metamorphic.
32. Position of anterior end of the ilium with respect to sacral diapophyses at the beginning of metamorphosis: (0) At the same level, (1) Anterior.
33. Position of ilium with respect to sacral diapophyses at the end of metamorphosis: (0) At the same level, (1) Anterior.
34. Spines of the presacral transverse processes: (0) Absent, (1) Present.
35. Vertebrae with the longest transverse process: (0) Sacral vertebra, (1) Vertebra III, (2) Sacral and vertebrae III, (3) Vertebrae III and IV.
36. Expansion of the sacral diapophyses: the opening angle of the distal edge of sacral diapophyses (Emerson, 1979): (0) Not expanded: 0° to 29.99°, (1) Lightly expanded: 30° to 49.99°, (2) Expanded: 50° to 89.99°, (3) Broadly expanded: 90° to 119.99°.

37. Orientation of the sacral diapophyses: angle between the longitudinal axis of the vertebral column and the transverse axis of the sacral diapophyses, measured from the middle sacral vertebral body, including cartilage: (0) Perpendicular to the axis of the body: (0) Perpendicular: 93° to 102.99°; (1) Slightly posterior: 103° to 112.99°; (2) Posterior: 90° to 109.99°.
38. Lateral processes of the urostyle: (0) Absent, (1) Present and rounded, (2) Present and spine-shaped, (3) Present and elongated.
39. Crest length of the urostyle relative to total length: (0) Less than 45%, (1) Between 45 and 65%, (2) Greater than 65%.
40. Sacro-urostyle joint: (0) Monocondylar, (1) Bicondylar.
41. Relationship between the condyles in the sacrum-urostyle joint: (0) Contiguous (1) Separated.
42. Coracoid position relative to the axis of the body: (0) Transverse, (1) Diagonal.
43. Ratio of coracoid length to height: (0) Less than or equal to twice its height: lower than 2.5; (1) Greater than twice its height: greater than or equal to 2.5.
44. Coracoid protuberance: (0) Absent, (1) Present.
45. Curvature of the clavicle: angle between the anterior distal end of the clavicle and the medial tip: (0) More curved or deep: greater than 70°, (1) Less curved or deep: lower than 70°.
46. Overlapping epicoracoids: (0) Right over left, (1) Left over right.
47. Joint of the glenoid fossa: (0) Synchondrotic, (1) Synostotic.
48. Crest on the anterior edge of the scapula: (0) Absent, (1) Present.
49. Ratio of proximal edge height to distal edge height (0) Distal and proximal edges of approximately the same height: 0 to 1.5; (1) Distal edge slightly higher than the proximal: 1.5 to 3; (2) Distal edge much higher than the proximal: 3 to 4.5.
50. Shape of the distal anterior edge of the suprascapula: (0) Convex, (1) Straight, (2) Concave.
51. Antero-distal projection of the suprascapula: (0) Absent, (1) Present.
52. Antero-lateral processes of the sternum: (0) Absent, (1) Present.
53. Number of sesamoids in the ilio-sacral joint: (0) One, (1) Two.
54. Acetabular joint: (0) Synchondrotic, (1) Synostotic, (2) Fused.
55. Shape of the dorsal posterior edge of the ischium: (0) Continuous/rounded, (1) Wide concavity, (2) Narrow concavity.
56. Angle between the ilial shaft and anterior edge of acetabular plate: (0) Obtuse: greater than 100°, (1) Straight: between 70° and 100°, (2) Acute: below 70°.
57. Groove of the pubis: (0) Absent, (1) Present.
58. Degree of calcification of the pubis: (0) Cartilaginous, (1) Partially calcified, (2) Completely calcified.
59. Length of anterior portion of the vertebral column (presacral + sacral vertebrae) relative to the pelvic girdle length. The length of the presacral + sacral vertebrae measured from the anterior end of the first vertebra to the sacro-urostyle joint. The length of the pelvic girdle was measured from the anterior end of the ilium to the posterior end of the ischium: (0) Vertebral column is shorter than the pelvic girdle, (1) Vertebral column and pelvic girdle are of the same length, (2) Vertebral column is longer than the pelvic girdle.
60. Form of the posterior edge of the sternum: (0) Single (1) Divided.
61. Ratio of length of scapula to clavicle length: (0) Scapula longer than clavicle: between 0.30 and 0.89, (1) Scapula and clavicle almost the same length: between 0.90 and 1.49 (2) Scapula shorter than the clavicle: between 1.50 and 2.09.
62. Ratio of width of the sacral diapophyses to width of the sacral vertebral body. (0) Sacral vertebral body wider than sacral diapophyses: lower than 0.7 (1) Sacral vertebral body and sacral diapophyses almost same width: between 0.7 and 1.4 (2) Sacral diapophyses wider than sacral vertebral body: greater than 1.4.
63. Shape of sesamoid of the ilio-sacral joint: (0) Rounded or trapezoidal, (1) Elongated.
64. Shape of procoracoid, in cross section, at the anterior end of the pectoral girdle (Fig. 9A,B): (0) Elongated, (1) Rounded.
65. Ligamentous tissue at the level of sternum (Fig. 9C,D): (0) Absent (1) Present.
66. Region of the ilium where the ligament of the ilio-sacral joint inserts (Fig. 9E,F): (0) Dorsomedial and ventro-lateral, (1) Medial and lateral, (2) The entire perimeter of the ilium (Manzano and Barg, 2005).
67. Thickest region of the ligament of the ilio-sacral joint (Fig. 9F): (0) Lateral, (1) Medial.
68. Ilium shape in cross section (Fig. 9F): (0) Elongated, (1) Rounded (Manzano and Barg, 2005).

A matrix was constructed with these data (supporting information Apendix III). In the phylogeny of Pyron and Wiens (2011), nine characters optimize as synapomorphies of groups: characters 35, state 0 (expansion of the sacral diapophyses: not expanded) grouped *T. ceiorum* with *T. atacamensis*. Character 28, state 1 (anteriorshape of ilium: curved and pointed) and 58, state 1 (length of the vertebral column relative to the pelvic girdle

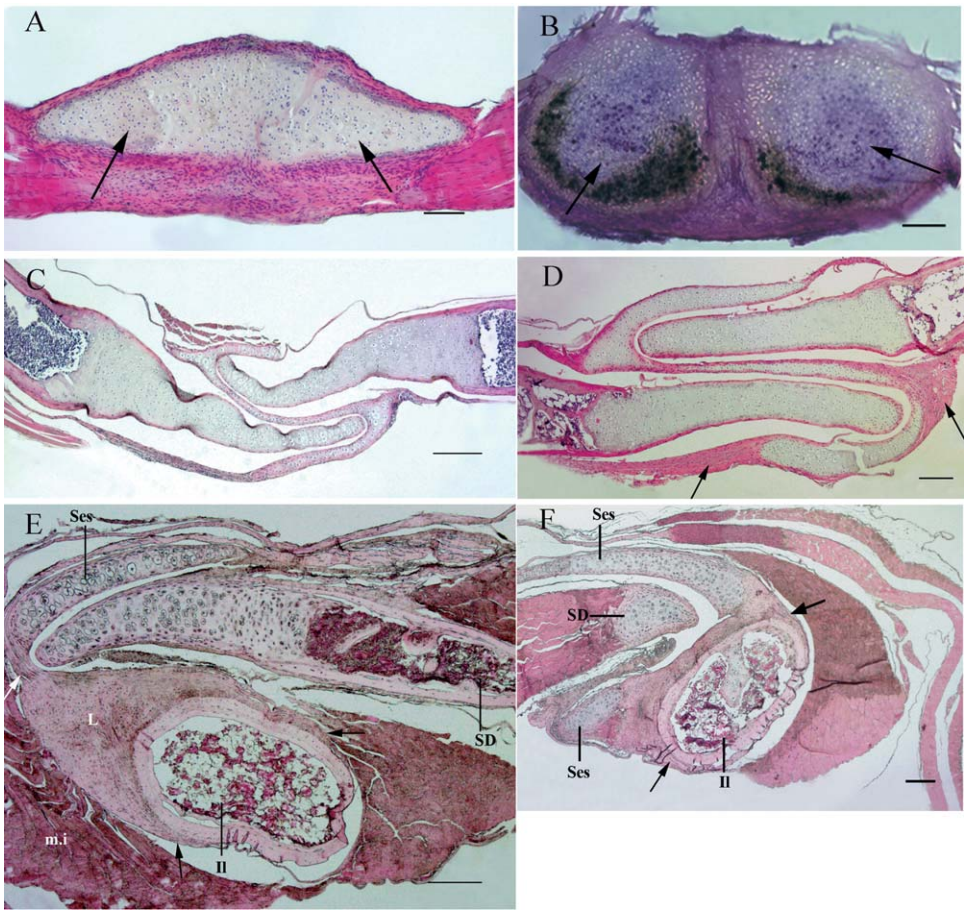

Fig. 9. (**A, B**) Histology of the adult anterior pectoral girdle; cross sections. Character 63, shape of procoracoid, in cross section, at the anterior end of the pectoral girdle. A: State 0, elongated procoracoides in *Phyllomedusa sauvagii*. B: State 1, rounded procoracoides in *Pseudis platensis*. The arrows indicate the procoracoid. Scale bars: 50 μm. (**C, D**) Histology of the adult pectoral girdle; cross-sections the sternum level. Character 64, ligamentous tissue at the level of sternum. C: State 0, absent in *Scinax fuscovarius*. D: State 1, present in *Phyllomedusa sauvagii*. The arrows indicate the ligamentous tissue. Scale bars: 100μm. **(E, F)** Histology of the adult ilio-sacral joint; cross sections. E: *Hypsiboas riojanus*, character 65 (0) the ligament of the ilio-sacral joint inserts in the dorso-medial and ventro-lateral region of the ilium, character 66 (0) thickest lateral region of the ligament of the ilio-sacral joint, character 67 (0) the ilium is elongated in cross section. **F**: *Phyllomedusa sauvagii*, character 65 (1) the ligament of the ilio-sacral joint inserts in the medial and lateral region of the ilium, character 66 (1) thickest medial region of the ligament of the ilio-sacral joint, character 67 (0) the ilium is elongated in cross section. The black arrows indicate the ligament insertion sites in the ilium, the white arrow the insertion site in the sesamoid. Scale bars: 100 μm. SD, sacral diapophysis; Il, ilium; L, ligament; m.i., *musculus ilioliumbaris*; Ses, sesamoid.

length: vertebral column and pelvic girdle are of the same length) grouped the clade [(*P. boliviana* (*P. sauvagii* + *P. tetraploidea*)]; character 52, state 1 (number of sesamoids in the iliosacral articulation: two) and 56, state 1 (groove of the pubis: present) grouped *P. sauvagii* and *P. tetraploidea*; the latter character reappeared at the base of the Hylinae clade. Character 33, state 0 (spines of the presacral transverse processes: present); character 44, state 1 (curvature of the clavicle: less curved or deep: lower than 70°); character 54, state 1 (form of the dorsal posterior edge of the ischium: wide concavity), and character 56, state 1 (Groove of the pubis, present) grouped the clade Hylinae. Forty four characters are autapomorphies of species (Fig. 10).

Some developmental characters show an interesting pattern. The characters one (beginning of chondrification of sacrum), two (beginning of chondrification of first pair of postsacral vertebrae), three (beginning of chondrification of girdles and limbs), and seven (beginning of ossification of coracoids) show a relatively retarded development in the walker-arboreal *Phyllomedusa* clade (Fig. 11). Characters two and three also show relatively delayed development in *S. fuscovarius* (jumper-arboreal). Characters three and seven present delayed development in *L. limellum* (swimmer-jumper; in water or aquatic vegetation; Fig. 11). Character 18, state 0 (position of hypochord-sacrourostyle joint at the end of stage 46: posterior) is optimized at the base of the Hylinae (jumper

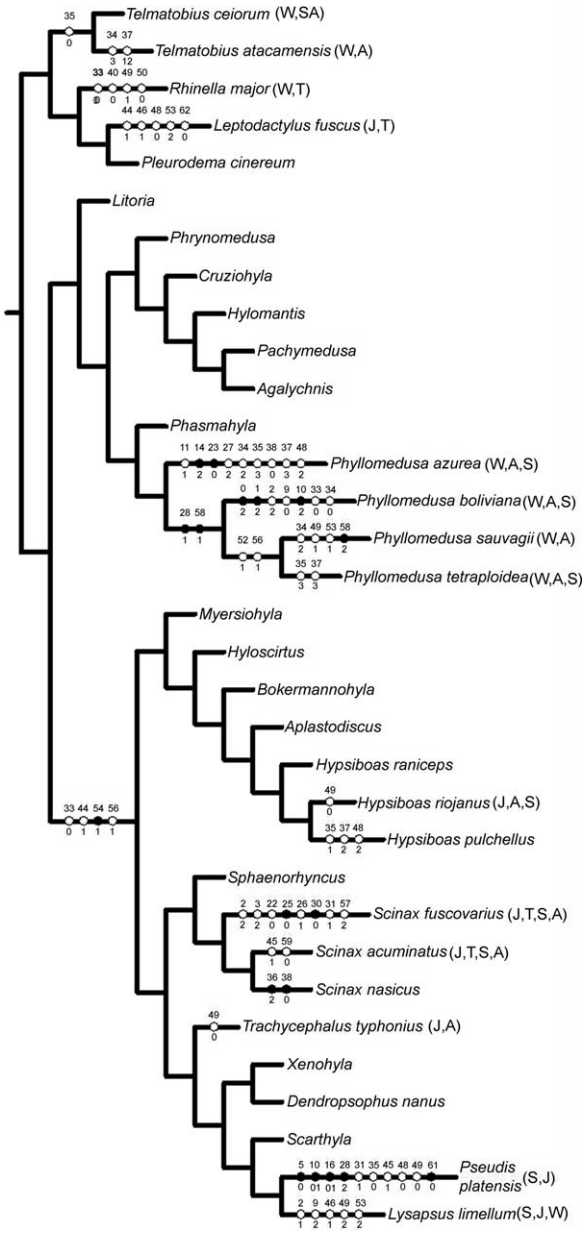

Fig. 10. Simplified anuran phylogeny of Pyron and Wiens (2011) showing the relationships of the analyzed taxa. The synapomorphies for each node are indicated on the cladogram. Numbers above nodes are character numbers. Numbers below nodes are the states of each character. Empty and solid hashmarks indicate homoplastic and nonhomoplastic characters, respectively. The locomotor modes and habitat of the species analyzed are in parenthesis: A, aquatic; J, jumper; SA, semiaquatic; S, shrubby; T, terrestrial; W, walker.

considering the species studied here) and state 1 (anterior position of hypochord-sacrourostyle joint at Stage 46) grouped the *Phyllomedusa* species (Fig. 12).

Among the characters of adults, character 34, state 3 (Vertebrae III and IV with the longest transversal process), which groups the aquatic species (*P. platesis* and *L. limellum*), is notable for its distribution (Fig. 12). Characters 35 (expansion of the sacral diapophyses) and 36 (orientation of the sacral diapophyses) show the biggest expansion in the arboreal-walker species *P. azurea* and *P. tetraploidea*; the former species shows a perpendicular position of the sacral diapophyses, a state that also is acquired in *D. nanus* (Fig. 12). Character 37 (lateral process of urostyle) shows a diverse configuration among the studied species; state 1 (present and rounded) grouped the clade of the swimmer-jumper species (*Pseudis* and *Lysapsus*); state two (present and spine-shaped) is optimized in *H. pulchellus* and at the base of the *Phyllomedusa* clade (Fig. 13). Character 39, state 0 (sacrum-urostyle joint: monocondylar; Fig. 13) and 59, state 0 (form of the posterior edge of the sternum: single) optimize at the base of the *Phyllomedusa* clade, and has independent acquisition in *S. acuminatus* and *D. nanus*, *R. major*, and *L. fuscus*. Character 41, state 0 (coracoid position relative to the axis of the body: perpendicular) is acquired in the *Scinax* clade. Character 44, state 1 (curvature of the clavicle: less curved or deep; Fig. 13) and 54, state 1 (angle between the ilial shaft and anterior edge of acetabular plate: wide concavity; Fig. 14) optimize at the base of the Hylinae clade (jumper for the species studied here). The first character appears independently in *L. fuscus* (Fig. 13), and the second character, state 2 (narrow concavity) is optimized at the base of the clade *Hypsiboas* (Fig. 14). Character 50, state 0 (antero-distal projection of the suprascapula: absent) grouped the species of *Phyllomedusa* and appeared independently in *R. major* (Fig. 14). Character 55, state 1 (angle between the ilial shaft and anterior edge of acetabular plate: Straight, between 70° and 100°) is optimized at the base of *Phyllomedusa* clade, *Telmatobius* clade and also in *L. fuscus*; state 2 (acute, lower than 70°) is optimized at the base of *Pseudis* + *Lysapsus* clade (Fig. 13). Character 57, state 0 (cartilaginous pubis) appears in the jumper-swimmer species (*P. platensis* and *L. limellum*). Character 62, state 0 (general shape of sesamoid of iliosacral articulation: rounded or trapezoidal) appears in *Scinax* clade and is independently acquired in *L. fuscus* (Fig. 14).

DISCUSSION

The results of the phylogenetic mapping show that nine osteological characters optimize as synapomorphies of groups, and 44 as autapomorphies. Among the latter, some characters related to developmental timing of skeletal elements defined species such as *P. platensis, L. limellum, P. azurea*, and *P. boliviana*. The relatively early beginning of chondrification and ossification of the hypochord are autapomorphies of *P. platensis*. In *P. azurea*, some events involved in the development of the girdle occur later than in the other species:

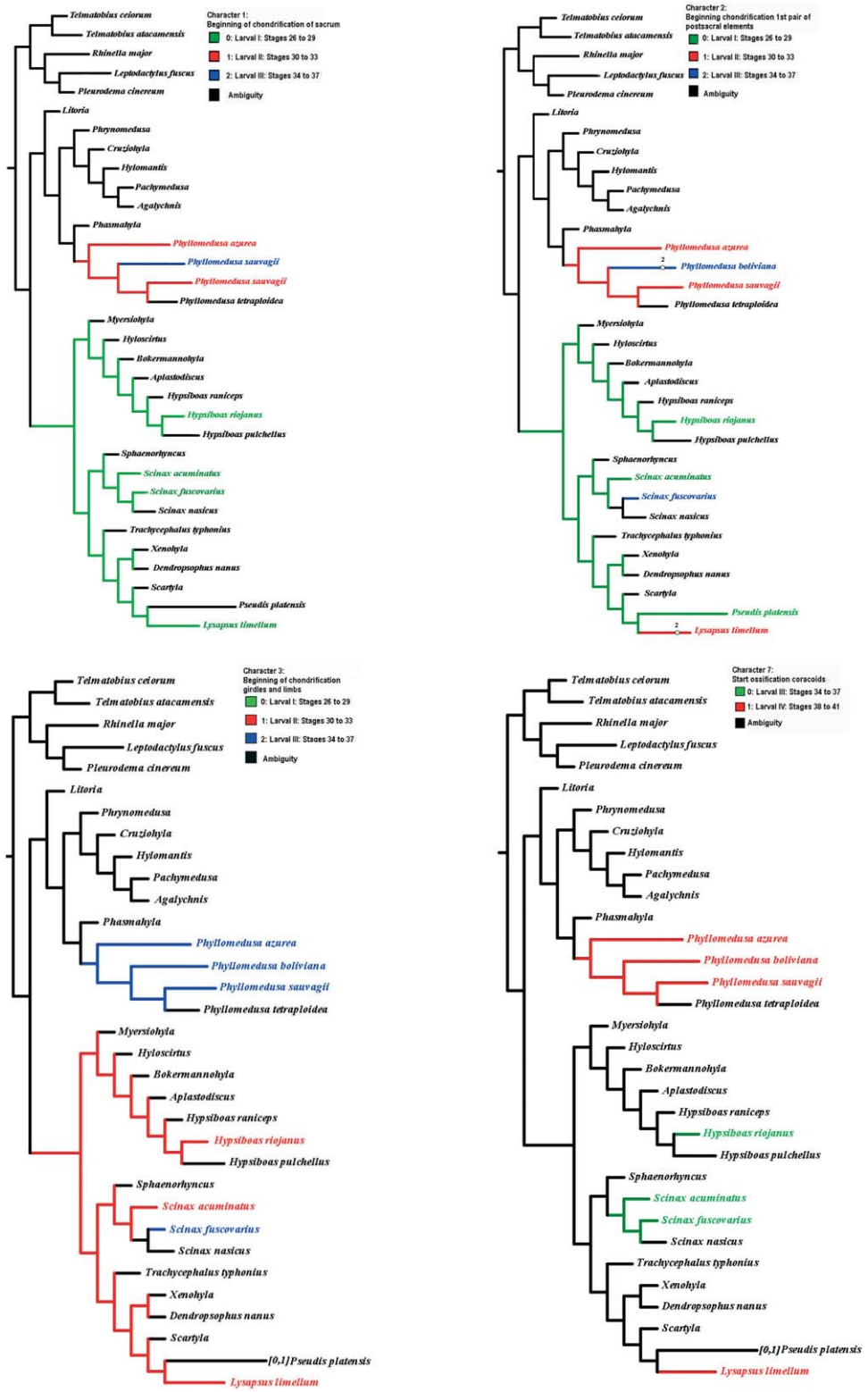

Fig. 11. Cladograms (from simplified anuran phylogeny of Pyron and Wiens, 2011) showing change of states in: Character one (Beginning of chondrification of sacrum), two (Beginning of chondrification first pair of postsacral vertebrae), three (Beginning of chondrification girdles and limbs) and seven (Beginning of ossification of coracoids).

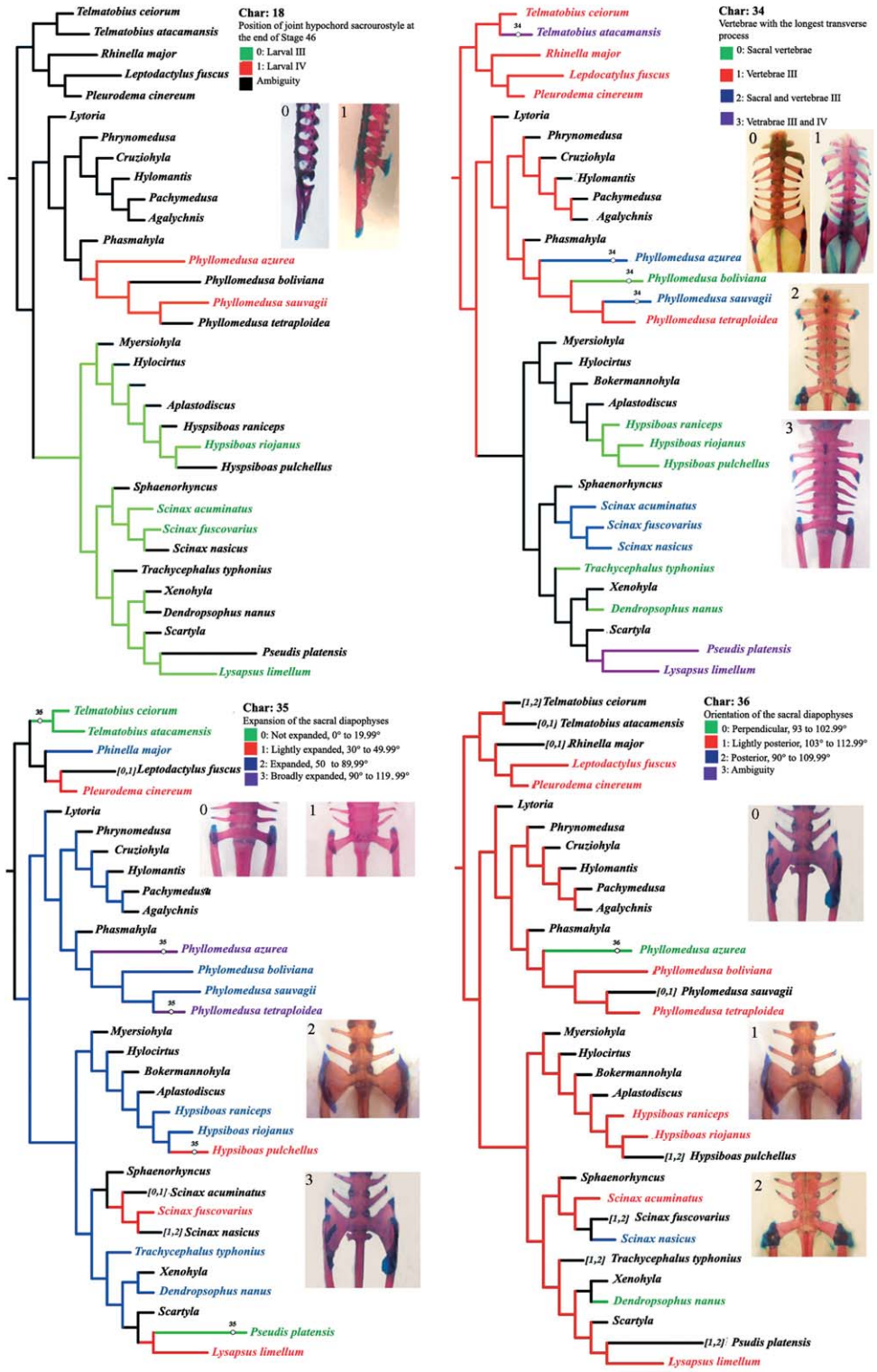

Fig. 12. Cladograms (from simplified anuran phylogeny of Pyron and Wiens, 2011) showing change of states in: Characters 18 (Position of hypochord-sacrourostyle joint at the end of Stage 46; state 0 in *Phyllomedusa boliviana*, state 1 in *Scinax nasicus*). Character 34 (Vertebrae with the longest transverse process); state 0 in *P. boliviana*; state 1 in *Phyllomedusa tetraploidea*; state 2 in *Scinax fuscovarius*; state 3 in *Pseudis platensis*. Character 35 (Expansion of the sacral diapophyses); state 0 in *P. platensis*; state 1 in *Lysapsus limellum*; state 2 in *Hypsiboas riojanus*; state 3 in *Phyllomedusa azurea*). Character 36 (Orientation of the sacral diapophyses); state 0 in *P. azurea*, state 1 in *H. riojanus*); state 2 in *S. fuscovarius*.

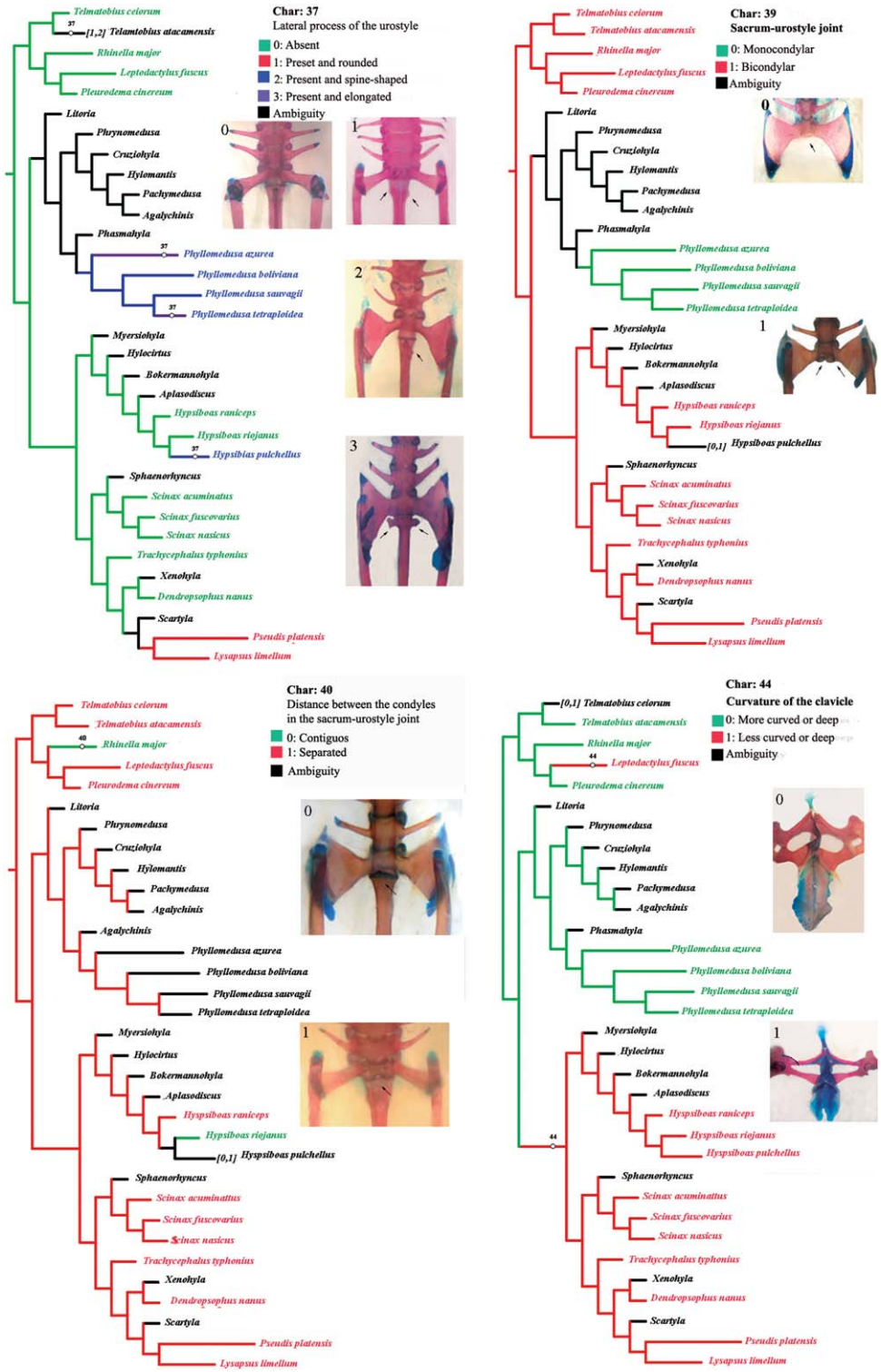

Fig. 13. Cladograms (from simplified anuran phylogeny of Pyron and Wiens, 2011) showing change of states in: Characters 37 (lateral process of the urostyle); state 0 in *Scinax acuminatus*; state 1 in *Lysapsus limellum*; state 2 in *Hypsiboas pulchellus*; state 3 in *Phyllomedusa azurea*. Character 39 (Sacrum-urostyle joint); state 0 in *Phyllomedusa sauvagii*; state 1 in *Hypsiboas riojanus*. Character 40 (Distance between the condyles in the sacrum-urostyle joint); state 0 in *H. riojanus*; state 1 in *L. limellum*). Character 44 (Curvature of the clavicle); state 0 in *Phyllomedusa boliviana*; state 1 in *L. limellum*. Character 40 (Distance between the condyles in the sacrum-urostyle joint); state 0 in *H. riojanus*; state 1 in *L. limellum*. Character 44 (Curvature of the clavicle); state 0 in *P. boliviana*, state 1 in *L. limellum*.

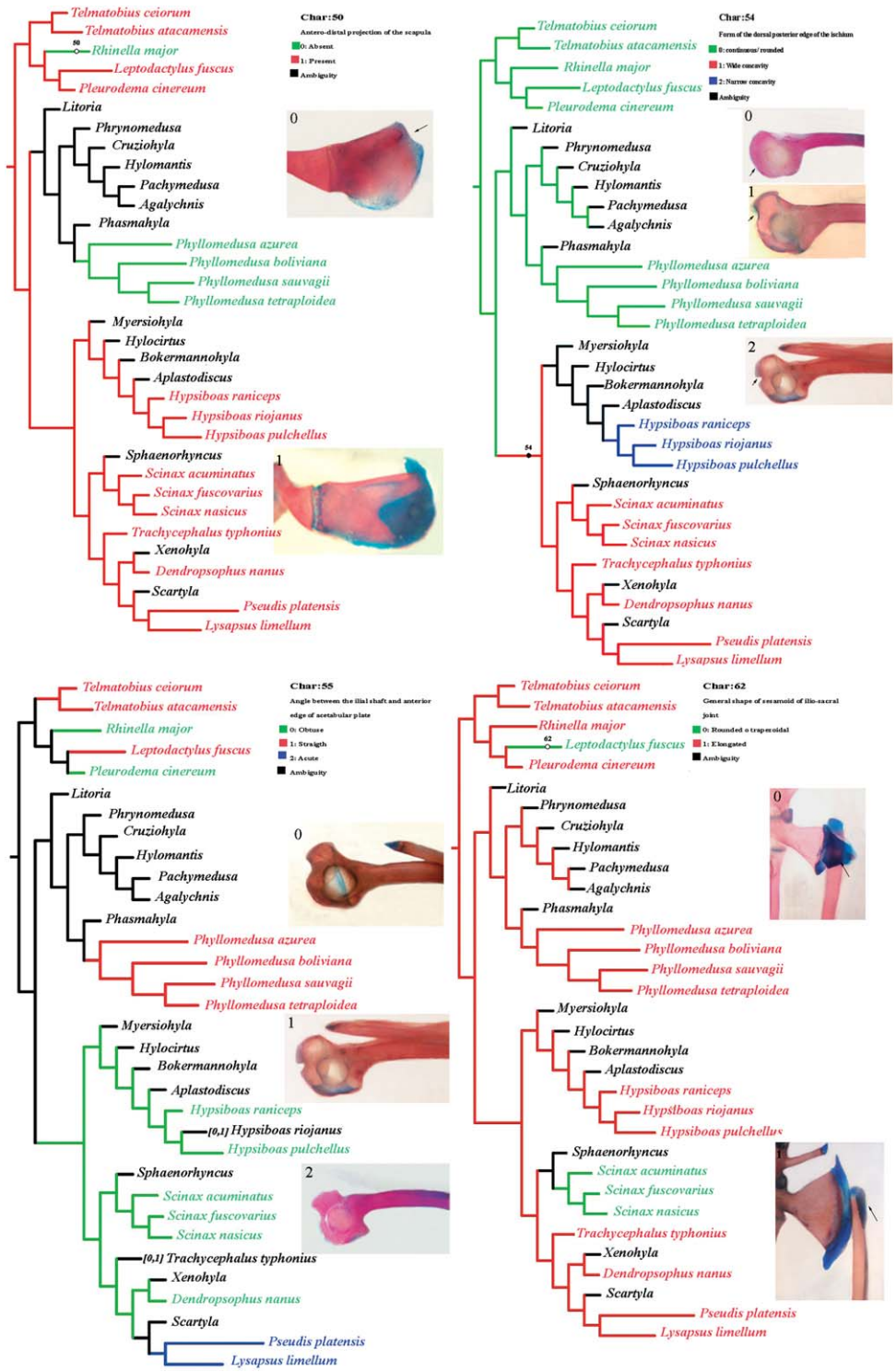

Fig. 14. Cladograms (from simplified anuran phylogeny of Pyron and Wiens, 2011) showing change of states in the characters 50 (Antero-distal projection of the suprascapula); state 0 in *Phyllomedusa boliviana*, state 1 in *Scinax nasicus*. Character 54 (Shape of the dorsal posterior edge of the ischium); state 0 in *Phyllomedusa tetraploidea*; state 1 in *Scinax fuscovarius*; state 2 *Hypsiboas raniceps*. Character 55 (Angle between the ilial shaft and anterior edge of acetabular plate); state 0 in *Dendropsophus nanus*; state 1 in *H. raniceps*; state 2 in *Lysapsus limellum*. Character 60 (Relationship between lengths of the scapula and clavicle); state 0 in *Scinax nasicus*, state 1 in *Hypsiboas riojanus*.

ossification of the clavicle and cleithrum, acquisition of the adult configuration in the posterior area of the pelvic girdle, and perpendicular position of femur. In *P. azurea*, the contact between both pelvic hemigirdles occurs earlier than in other species. In *P. boliviana*, the beginning of chondrification of presacral vertebrae, sacrum, and the first pair of postsacral vertebrae occurs in later stages that the other studied species. In summary, the developmental timing of chondrification, ossification and differentiation of axial and girdle skeleton show interspecific and intercharacter variation. Haas (1999) found a similar pattern in other species, concluding that although the skeletal differentiation seems conservative in the larval development of anurans, there are specific (autapomorphies) variations in some lineages. All the species seem to converge in the same degree of differentiation of the axial and appendicular skeleton at the end of the metamorphosis, because of the mechanic constraints imposed by the terrestrial life (Haas, 1999). Many of the studied characters fit this concept, but not all of them. For example, the sesamoids are present at the ilium-sacral joint in *S. fuscovarius* and *S. acuminatus* throughout metamorphosis, but in *H. riojanus*, *P. sauvagii*, *P. azurea*, and *L. limellum*, they are absent in the metamorphic period but present in the adults. This example shows that the postmetamorphic period is also fundamental to the complete differentiation of structures related to a full locomotor functionality (Vera and Ponssa, 2014).

In the pelvic girdle, the time of ossification of the scapula, clavicle, cleithrum and coracoids also varies among species. In *H. riojanus* (jumper, arboreal-shrubby), these elements ossified during the larval period III. In *P. sauvagii* (walker-arboreal), the scapula, clavicle and cleithrum ossify during the larval period III, and the coracoids in the larval period IV. In *L. limellum* (swimmer–jumper, in water and aquatic vegetation), ossification of these elements occurs later than in the other species, during the larval period IV. Similarly, in the aquatic species *Xenopus laevis*, *Discoglossus sardus*, and *Bombina orientalis*, ossification of the scapula occurs later than in other elements of the pelvic girdle and even later than in nonaquatic species (Haas, 1999). The observed variation in the timing of some developmental processes highlights the importance of analyzing this topic within the frame of heterochrony, which is a main factor driving morphological differentiation in anurans (Manzano et al., 2013).

The iliosacral articulation forms throughout metamorphosis (Stages 42–46) in all the studied species, as in *Rana temporaria* (Pomikal et al., 2011). A feature linked with the formation of this joint is the position of the anterior end of ilium relative to the sacral diapophyses. The position of the pelvis and axial skeleton throughout development would be associated with the ilio-sacral articulation-type in the adult (Ročková and Roček, 2005). According to Ročková and Roček (2005), an ilium at the level of the sacral diapophyses would be associated with aquatic species such as *Bombina* and *Xenopus*. Nevertheless, we observed the ilium at the level of the sacral diapophyses in species with different locomotor modes and habitats, for example, *Lysapsus limmellum* (swimmer–jumper, in water and aquatic vegetation), *H. riojanus* and *T. typhonius* (jumper, arboreal–shrubby), *P. sauvagii* and *P. azurea* (walker, shrubby).

A character highly linked with the specialized jumping mode of anurans is found in the sacro-urostylic region, whose transformation is unique among tetrapods (Púgener and Maglia, 2009). Good jumper anurans have a very flexible iliosacral articulation (Green, 1931) with anteroposterior and rotational movements that, together with the sacral-urostylic articulation, align the vertebral column with the pelvic girdle during jumping (Jenkins and Shubin, 1998; Kargo et al., 2002). Some authors consider that aquatic anurans have a movement and a postcranial skeleton design similar to those of specialist jumpers, propelling themselves with a kick (Gans and Parsons, 1966; Emerson, 1982). However, Abourachid and Green (1999) state that those locomotor modes could be independently derived locomotor trends. The variation observed in the sacral-urostylic articulation is the result of different pathways in taxa with diverse life histories (Púgener and Maglia, 2009). Here, we observed two slightly different modes of development of the sacro-urostylic joint. In one of them, during metamorphosis the hypochord migrates dorsally and its anterior end fuses with the first vertebra, and does not exceed the sacral-urostylic joint, resulting in a bicondylar articulation. The latter is present in jumper species: *S. fuscovarius* (terrestrial, shrubby, arboreal), *S. acuminatus* (terrestrial, shrubby, arboreal), *H. riojanus* (arboreal, shrubby), *T. typhonius* (arboreal), and *L. limellum* (water and aquatic vegetation). Púgener and Maglia (2009) observed this developmental pathway in jumper-terrestrial species (i.e., *Acris crepitans* and *D. sardus*), it would be the most generalized mode according the optimization found here, and the pattern described in other taxa such as *Ascaphus truei*, *B. orientalis*, *Ceratophrys ornata*, *Hyloxalus subpunctatus*, *Gastrophryne carolinensis*, *Hypsiboas lanciformis*, *Rhinophrynus dorsalis* (Púgener and Maglia, 2009), *Ceratophrys cornuta* (Wild, 1997), *Phyllomedusa vaillantii* (Sheil and Alamillo, 2005), and *Pyxicephalus adspersus* (Sheil, 1999). In the other developmental pathway, the anterior end of the hypochord extends up to the level of the iliosacral articulation, resulting in a monocondylar joint in the adult. This mode is present in the walker–arboreal, shrubby species *P. azurea* and in the walker-arboreal *P. sauvagii*.

Púgener and Maglia (2009) described this mode for hopper-burrower species, *Spea multiplicata*, and aquatic species, *X. laevis*. A similar pattern has been identified in other taxa with fused sacrum and urostyle, such as *Pipa pipa* (Trueb et al., 2000), *Scaphiopus couchii* (Púgener and Maglia, 2009), and *S. bombifrons* (Wiens, 1989). The convergence in the developmental mechanism in species with three different particular locomotor modes (walker, swimmer, and burrower) shows how different challenge mechanics are resolved through similar developmental pathways. In our optimization, the basal state is a bicondylar iliosacral articulation, the monocondylar condition optimized at the base of the *Phyllomedusa* clade. Bicondyly would be more appropriate for jumping, as it appears to be uniaxial, with movement restricted to axial flexion-extension (Púgener and Maglia, 2009; Reilly and Jorgensen, 2011). Reilly and Jorgensen (2011) propose that bicondyly or urostylic fusion (or both) provide limited urostylic mobility in the lateral direction, and it would have appeared as an adaptation to burrow/lateral-bending (and walking) locomotion, being an exaptation to sagittal-hinge jumping that appears in the Neobatrachia. Other neobatrachian walker/hoppers show expanded bicondyly and sacral diapophyses (i.e., Myobatrachidae, Cycloramphidae, some Microhylidae; Reilly and Jorgensen, 2011). The jumper species of the hylinae clade show bycondily, which aligns the vertebral column with the pelvic girdle during jumping (Jenkins and Shubin, 1998; Kargo et al., 2002). Jenkins and Shubin (1998) concluded that a bicondylar articulation is the best joint for saltatorial locomotion because it restricts movement to a hinge-like flexion/extension, and that other kinds of joints are found in species in which jumping is not the main mode of locomotion. The lateral-bender morph (implying monocondyly) and the walker/hopper locomotor mode are the basal condition for the Anura (Reilly and Jorgensen, 2011). This joint would have the freedom of three-dimensional movements (Reilly and Jorgensen, 2011). In hylids, the walker clade *Phyllomedusa* shows monocondylar sacral-urostylic joint, which would allow lateral bending, and retains the basal condition of expanded sacral diapophyses (with greater expansion in two species, as discussed below), which would allow fore-aft-sliding (Reilly and Jorgensen, 2011).

Together with the iliosacral articulation, the muscles *ilio-lumbaris* and *longissimus dorsi* are the responsible for the rotation of the pelvis through locomotion (Emerson, 1979; Jenkin and Shubin, 1998). The *ilio-lumbaris* originates on the anterolateral tip of the ilium (Emerson, 1979) or on the ligamentous cap, from the anterior region of the iliac crest and inserts on the lateral processes of the presacral vertebrae IV–VIII (Emerson, 1982; Manzano and Barg, 2005). The longer presacral transverse processes of vertebra IV of *P. platensis* and *L. limellum* would provide greater surface for muscular insertion. Actually, Emerson (1982) observed that longer presacral transverse processes are associated with vertical rotation of the pelvis.

The expansion of the sacral diapophyses has also been considered a feature linked with locomotor capacities in anurans (Emerson, 1979, 1982; Simon, 2008; Jorgensen and Reilly, 2013). Thus, greatly expanded flat-sided sacral diapophyses are proposed to be a fore-aft-sliding system in aquatic, climbing, and burrowing forms. A bowtie-like sacrum and narrow to moderately expanded sacral diapophyses is a lateral-bending system in walker/hoppers and some burrowers (Emerson, 1979). A third system, with rod-like, nonexpanded diapophyses would function as a sagittal-hinge system, limiting the iliosacral movement to vertical rotation in long-distance jumpers (Emerson, 1979). It is accepted that the basal condition for frogs is expanded sacral diapophyses, a state that is present in the basal taxa *Ascaphus* and *Prosalirus* (Reilly and Jorgensen, 2011). It has also been mentioned as the general condition across anurans (Reilly and Jorgensen, 2011). In our analysis of the Hylid clade, an expanded diapophysis also is the basal state. The optimization showed that bigger expansion of the sacral diapophysis is a derivate condition present in two walker-arboreal species, *P. azurea* and *P. tetraploidea*. A similar pattern was described by Jorgensen and Reilly (2013), who found that members of the subfamily Hylinae show moderately expanded sacral diapophyses and those of the subfamily Phyllomedusinae show larger diapophyseal expansion. Nonexpanded diapophyses are optimized at the base of the clade of walker-aquatic species, *T. ceiorum* and *T. atacamensis*, and in the swimmer and jumper-aquatic species *P. platensis*. Similarly, Simons (2008) found that the arboreal hylids *Hyla versicolor* and *Osteopilus vastus* show greater expansion in the sacral diapophyses than swimmer hylids, such as *Pseudis paradoxa*. Jorgensen and Reilly (2013) proposed that burrower-walker-hopper and walker-hopper frogs tend to have relatively greater diapophyseal expansion than jumping frogs. These authors suggest that a hypothesized increase in lateral-bending ability given by greater diapophyseal expansion may support the walker behavior. Accordingly, two walker–arboreal species resulted with the greatest expansion in the sacral diapophyses (*P. azurea* and *P. tetraploidea*). Nevertheless, the smaller expansion is found in two walkers (both *Telmatobius* spp.) and in one jumper species (*P. platensis*), the three cases being aquatic species. Consequently, considering our analysis level, the morphological convergence of narrow sacral diapophyses seems to be related to the aquatic habitat more than to a kind of locomotor mode.

In Emerson's (1979) definition of the types of articulations, three elements are involved: the extension of the sacral diapophyses, the position and shape of the sesamoids, and the origin and

insertion of the articular ligaments. Actually, the origin and insertion of the articular ligaments are decisive in the functional interpretation of the patterns of sacral articulation (Emerson, 1979). Although the histological characters are only available for a limited sample, it is noticeable that three observed species show differences in the location of the ilial insertion of the ligament of the iliosacral articulation, that is, medial and lateral zone in *P. sauvagii*, dorso-medial and ventro-lateral in *H. riojanus*, in the entire perimeter of the ilium in *L. limellum*. The other included character (thickest region of ligament of the ilio-sacral joint) shows differences in the configuration observed between the two species of Hylinae analyzed (thickest region: lateral) and *P. sauvagii* (thickest region: medial). The types of articulation noted by Emerson (1979) make reference to the insertion of the ligament on the sacral diapophyses surface, whereas we observed differences in the ilial insertion. The morphological variability along with the differences in mechanical challenge of the different locomotor modes of the studied species suggests the need for a deeper functional analysis, since it is known that properties of the ligament facilitate the transmission and dissipation of forces across the composite structure, allowing skeletal loading (Doschak and Zernicke, 2005). Thus, location and bigger volume could represent a differential stress in different areas of the articulation, implying variation in the mechanical function; more samples and functional analyses are necessary to test this hypothesis.

Besides the degree of sacral expansion, the iliolumbaris muscle and the articular ligament, sesamoid shape and size also determine the direction of movement at the iliosacral articulation of a frog. The shape of the articular sesamoids is not easily quantifiable (Emerson, 1982). In our optimization, the most generalized shape is an elongate sesamoid, a rounded sesamoid optimizes at the base of the *Scinax* clade and is convergent in *L. fuscus*. The presence of a sesamoid would be associated with lateral and vertical rotation, whereas its absence would correspond to the antero-posterior movement in the horizontal plane. In the aquatic species of hylids, *L. limellum* and *P. platensis*, articular sesamoids were described as associated with the ligaments of the articular capsule (Manzano and Barg, 2005). This capsule could increase the range and angle of articulation during the transition from resting to swimming, acting as a turning point and adding freedom to the movement of rotation (Manzano and Barg, 2005). The histological data reveal a similar ligamentous capsule in *H. riojanus*, so it would not be unique to Pseudines. The presence of two sesamoids in some species, such as *P. sauvagii* and *P. tetraploidea*, and in the *Scinax* clade, would limit the lateral and vertical rotation movement required for jumping. Even when this character shows convergence in these clades (*Phyllomedusa* and *Scinax*), suggesting adaptation, it is noticeable that the *Scinax* clade optimizes with two derived sesamoids characters: the presence of two sesamoids, one of them notably elongated. These characters, together with the perpendicular position of the coracoids (Character 41), define this clade.

Among the characters of the pectoral girdle the most suggestive are: lesser curvature of the clavicle, which define the Hylinae clade; and clavicle larger than the scapula, which is present in the aquatic species *L. limellum* and some *P. platensis*. The *Pseudis + Lysapsus* clade is also defined by a cartilaginous pubis. The pubis was ossified in adults of early amphibians (Ročkova and Roček, 2005), and was separated from ischium and ilium by sutures in advanced forms (e.g., in the Permian *Archeria*; Romer, 1957). However, its development is arrested at the cartilaginous stage in anurans, except in Pipidae, Ascaphidae and Leiopelmatidae (Ročkova and Roček, 2005). Similarly, in the "aquatic clade" of hylids, the skeletogenesis of the pubis is arrested at a cartilaginous stage. Ossification seems to be highly variable even within a single species (Ročkova and Roček, 2005). Nevertheless, it is noticeable that the species whose habitat (water) is 900 times denser and 80 times more viscous than earth (Vogel, 1994) shows a lighter pubis, which could be imply a morphological consequence of the mechanical challenge. Another character that could be associated with the aquatic habitat is the antero-lateral process of the sternum, which appears in the *Pseudis + Lysapsus* clade and is convergent in the aquatic clade of *Telmatobius*.

The distribution of the character "crest on the anterior edge of the scapula" is very suggestive, as it is optimized in arboreal species (*P. boliviana*, *P. sauvagii*, *P. tetraploidea* and *T. typhonius*) and is convergent in aquatic species (*P. platensis* and *L. limellum*). A similar morphology appears to resolve the challenges of two different locomotor modes.

The axial and appendicular morphology of hylids has characters that relate to the locomotor function. For example, the aquatic species show greater vertebral body, longer and medially higher coracoids, and more concave and longer clavicles. The arboreal species show expanded sacral diapophyses and monocondylar sacrum-urostyle articulation. The aquatic species present a cartilaginous pubis, clavicle larger than scapula, and lateral process of the urostyle. The functional interpretations are quite particular to this family. The monophyletic clades (i.e., clades with a common evolutionary history) are precisely the groups with locomotor mode or habitats in common. For instance, swimming hylids exhibit significantly wider sacral vertebra than arboreal hylids, and arborealists exhibit significantly greater angle of sacral diapophyses than swimming species in this family (Simon, 2008). Because an inherited character implies that functional constraints could also be inherited the

variability that we see indicates that more investigation is needed to resolve the question of phylogeny or ecology. There is no clear indication that the morphological pattern has always happened in one way or the other, and variability rather than inviolate rules should often be expected.

ACKNOWLEDGMENTS

Susana Mangione helped us in the production of the histological data. For helpful for improving the English language, we thank James Menzies (SSAR Manuscript Review Service). To Diego Baldo for loan specimens.

LITERATURE CITED

Abourachid A, Green DM. 1999. Origins of the frog-kick? Alternate-leg swimming in primitive frogs, families Leiopelmatidae and Ascaphidae. J Herpetol 33:657–663.

Baleeva NV. 2001. Formation of the scapular part of the pectoral girdle in anuran larvae. Russian J Herpetol 8:195–204.

Baleeva NV. 2009. Formation of the coracoid region of the anuran pectoral girdle. Russian J Herpetol 16:41–50.

Cei JM. 1980. Amphibians of Argentina. Monitore Zoologico Italiano. Nuova Serie, Monographia. Firenze 2: ixii + 609.

Doschak MR, Zernicke RF. 2005. Structure, function and adaptation of bone-tendon and bone-ligament complexes. J Musculoskelet Neuronal Interact 5:35–40.

Duellman WE. 2001. The hylid frogs of Middle America. Society for the Study of Amphibians and Reptiles, Vol. 2. New York: Ithaca. p. 1180.

Emerson SB. 1979. The ilio-sacral articulation in frogs: Form and function. Biol J Linn Soc 11:153–168.

Emerson SB. 1982. Frog Postcranial morphology: Identification of a functional complex. Copeia 3:603–613.

Emerson SB. 1984. Morphological variation in frog pectoral girdles: Testing alternatives to a traditional adaptive explanation. Evolution 38:376–388.

Emerson SB. 1988. Convergence and morphological constraint in frogs: Variation in postcranial morphology. Fieldiana Zool 43:1–19.

Emerson SB, De Jongh HD. 1980. Muscle activity at the iliosacral articulation of frogs. J Morphol 166:129–144.

Fabrezi M. 2011. Heterochrony in growth and development in anurans from the Chaco of South America. Evol Biol 38: 390–411.

Fabrezi M, Goldberg J. 2009. Heterochrony during skeletal development of *Pseudis platensis* (Anura Hylidae) and the early offset of skeletal development and growth. J Morphol 270:205–220.

Fabrezi M, Manzano A, Lobo F, Abdala V. 2014. Anuran locomotion: Ontogeny and morphological variation of a distinctive set of muscles. Evol Biol 41:308–326.

Faivovich J, Haddad CFB, García PCA, Frost DR, Campbell JA, Wheeler WC. 2005. Systematic review of the frog family Hylidae, whit special reference to Hylinae: Phylogenetic analysis and taxonomic revision. Bull Am Mus Nat Hist 294:1–240.

Gallardo JM. 1993. Los anfibios de dos ecosistemas argentinos: Algunas estrategias en la reproducción y el desarrollo. Bol Soc Zool Uruguay 8:33–36.

Gans C, Parsons TS. 1966. On the origin of the jumping mechanism in frogs. Evolution 20:92–99.

Goloboff PA, Farris JS, Nixon KC. 2008. TNT, a free program for phylogenetic analysis. Cladistics 24:774–786.

Gosner KL. 1960. A simplified table for staging Anuran embryos and larvae with notes on identification. Herpetologica 16:183–190.

Green TL. 1931. The pelvis of the Anura. On the pelvis of the Anura: A study in adaptation and recapitulation. Proc Zool Soc 1931:1259–1290.

Haas A. 1999. Larval and metamorphic skeletal development in the fast-developing frog *Pyxicephalus adspersus* (Anura, Ranidae). Zoomorphology 119:23–35.

Heyer WR, Donnelly MA, Mc Diarmid RW, Foster MS. (Eds.). 2001. Medición y Monitoreo de la Diversidad Biológica. Universitaria de la Patagonia, p. 349.

Jenkins FA, Shubin NH. 1998. *Prosalirus bitis* and the anuran caudopelvic mechanism. J Vert Paleontol 18:495–510.

Jorgensen ME, Reilly SM. 2013. Phylogenetic patterns of skeletal morphometrics and pelvic traits in relation to locomotor mode in frogs. J Evol Biol 26:929–943.

Kaplán M. 2000. The pectoral girdles of *Rana rugulosa* (Ranidae) and *Nesomantis thomasseti* (Sooglossidae). Herpetologica 56:188–195.

Kaplán M. 2004. Evaluation and redefinition of the states of anuran pectoral girdle architecture. Herpetologica 60:84–97.

Kargo WJ, Nelson F, Rome LC. 2002. Jumping in frogs: Assessing the design of the skeletal system by anatomically realistic modeling and forward dynamic simulation. J Exp Biol 205: 1683–1702.

Lavilla EO. 1988. The genus Telmatobius (Anura: Leptodactylidae) and its relations with montane wetlands. In: Dalrympe GH, Loftus WF, Bernardino FS, editors. Wildlife in the Everglades and Latin America Wetlands, Miami: Florida International University. pp. 16–17 (english) and pp. 51–52 (spanish).

Lavilla EO, Barrionuevo JS. 2005. El género *Telmatobius* (Anura: Leptodactylidae) en la república Argentina: una síntesis. In: Lavilla EO, De la Riva I, editors. Estudios sobre las ranas andinas de los géneros *Telmatobius* y Batrachophrynus (Anura: Leptodactylidae). Valencia, España: Asociación Herpetólogica Española. Monografías de Herpetología 7. pp. 115–165.

Maglia AM, Púgener LA, Mueller JM. 2007. Skeletal morphology and postmetamorphic ontogeny of *Acris crepitans* (Anura: Hylidae): A case of miniaturitation in frogs. J Morphol 268: 194–223.

Manzano AS, Barg M. 2005. The iliosacral articulation in Pseudinae (Anura: Hylidae). Herpetologica 61:259–267.

Manzano AS, Baldo D, Barg M. 2004. Anfibios del litoral fluvial argentino. Miscelánea 12:271–290.

Manzano A, Abdala V, Ponssa ML, Soliz M. 2013. Ontogeny and tissue differentiation of the pelvic girdle and hind limbs of anurans. Acta Zool (Stockholm) 94:420–436.

Mc Diarmid RW, Altig R (Eds.). 1996. Tadpoles, The University of Chicago Press. p. 418.

Nixon KC. 2002. Winclada (BETA) Verion 1.00.08. Ithaca, NY: Nixon.

Pombal JP-JR, Haddad CFB. 1992. Especies de *Phyllomedusa* do grupo *burmeisteri* do Brasil oriental, com descrição de uma especies nova (Amphibia, Hylidae). Rev Bras Biol 52:217–229.

Pomikal C, Blumer R, Streicher J. 2011. Four-dimensional analysis of early pelvic girdle development in *Rana temporaria*. J Morphol 272:287–301.

Ponssa ML. 2008. Cladistic analysis and osteological descriptions of the frog species in the *Leptodactylus fuscus* species group (Anura, Leptodactylidae). J Zool Syst Evol Res 46:249–266.

Ponssa ML, Goldberg J, Abdala V. 2010. Sesamoids in anurans: New data, old issues. Anat Rec 293:1646–1668.

Přikryl T, Aerts P, Havelková P, Herrel A, Roček Z. 2009. Pelvic and thigh musculature in frogs (Anura) and origin of anuran jumping locomotion. J Anat 214:100–139.

Púgener LA, Maglia AM. 2009. Develpmental evolution of the anuran sacro-urostylic complex. South Am J Herpetol 4:193–220.

Pyron RA, Wiens JJ. 2011. A large-scale phylogeny of Amphibia including over 2800 species, and a revised classification of extant frogs, salamanders, and caecilians. Mol Phylogenet E 61:543–583.

Rage JC, Roček Z. 1989. Redescription of *Triadobatrachus massinoti* (Piveteau, 1936) an anuran amphibian from the early Triassic. Palaeontographica 206:1–16.

Reilly SM, Jorgensen ME. 2011. The evolution of jumping in frogs: morphological evidence for the basal anuran locomotor condition and the radiation of locomotor systems in crown group anurans. J Morphol 272:149–168.

Ročková H, Roček Z. 2005. Development of the pelvis and posterior part of the vertebral column in the Anura. J Anat 206:17–35.

Romer AS. 1957. The appendicular skeleton of the permian embolomerous amphibian *Archeria*. Contributions from the Museum of Paleontology, Vol. 13, University of Michigan. pp. 103–159.

Sheil CA. 1999. Osteology and Skeletal Development of *Pyxicephalus adspersus* (Anura: Ranidae: Raninae). J Morphol 240: 49–75.

Sheil CA, Alamillo H. 2005 Osteology and skeletal development of *Phyllomedusa vaillanti* (Anura: Hylidae: Phyllomedusinae) and a comparison of this arboreal species with a terrestrial member of the genus. J Morphol 265:343–368.

Shearman RM. 2005Growth of the pectoral girdle of the leopard frog, *Rana pipiens* (Anura: Ranidae). J Morphol 264:94–104.

Simons VFH. 2008. Morphological correlates of locomotion in anurans: Limb length, pelvic anatomy and contact structures, Thesis. Athens: College of Arts and Sciences of Ohio University.

Totty BA. 2002. Mucins. In: Bancroft JD, Gamble M, editors. Theory and Practice of Histological Techniques. Churchill: Livingston. pp. 163–200.

Trueb L. 1973. Bones, frogs, and evolution. In: Vial JL, editor. Evolutionary Biology of Anurans: Contemporary Research on Major problems. Columbia: University of Missouri Press. pp. 64–132.

Trueb L, Púgener LA, Maglia AM. 2000. Ontogeny of the bizarre: An osteological description of *Pipa pipa* (Anura: Pipidae), with an account of skeletal development in the species. J Morphol 243:75–104.

Van Dijk DE. 2002. Longitudinal sliding articulations in pipid frogs. South African J Sci 98:555–556.

Vellard J. 1954. Études sur le lac Ticicaca et Les *Telmatobius* du haut-plateau interandin. Javier Prado: Mem Mus Hist Na. p. 157.

Vera MC, Ponssa ML. 2014. Skeletogenesis in anurans: cranial and postcranial development in metamorphic and postmetamorphic stages of *Leptodactylus bufonius* (Anura, Leptodactylidae). Acta Zool 95:44–62. (Stockholm)

Vogel S. 1994. Life in Moving Fluids: The Physical Biology of Flow. Princeton, NJ: Princeton University Press. p. 488.

Wassersug RJ. 1976. A procedure for differential staining of cartilage and bone in whole formalin-fixed vertebrates. Stain Technol 51:131–134.

Wells KD. 2007. The ecology and behavior of Amphibians. Chicago: The University of Chicago press. p. 1085.

Wiens JJ. 1989. Ontogeny of the skeleton of *Spea bombifrons* (Anura: Pelobatidae). J Morphol 202:29–51.

Wiens JJ, Kuczynski CA, Hua X, Moen DS. 2010. An expanded phylogeny of treefrogs (Hylidae) based on nuclear and mitocondrial sequence data. Molec Phylogenet E 55:871–882.

Wilcox D, Dove B, Mc David D, Greer D. 2002. UTHSCSA Image Tool. Version 3.00. Univ. Texas Health Sc. Center San Antonio.

Wild ER. 1997. Description of the adult skeleton and developmental osteology of the hyperossified horned frog, *Ceratophrys cornuta* (Anura: Leptodactylidae). J Morphol 232: 169–206.